Computational kinematics of multibody systems: two formulations for a modular approach based on natural coordinates

M. Saura[a,*], P. Segado[a], D. Dopico[b]

[a]*Department of Mechanical Engineering. Universidad Politecnica de Cartagena. Doctor Fleming, s/n, 30202 Cartagena, Spain*
[b]*Mechanical Engineering Laboratory. University of A Coruña. Mendizabal, s/n, 15403 Ferrol, Spain*

Abstract

Multibody systems can be divided into an ordered set of kinematically determined modules, known as structural groups, in order to compute their kinematics more efficiently. In this work a procedure for the kinematic analysis of any kind of structural group is introduced, and two different methods for their solution in natural coordinates are presented: the time derivative (TD) and the third-order tensor (3OT) approaches. Moreover, the newly derived methods are compared in terms of efficiency with a global formulation, consisting in solving the kinematics of the multibody system as a whole using dense and sparse solvers. Two scalable case studies have been considered: a 2D four-bar linkage and a 3D slider-crank mechanism with an increasing number of constraint equations. The results show that the TD approach performs better in all cases with speed ups in a range of 27 to 61 times faster in 2D, and of 2.3 to 3.7 times faster in 3D with respect to the global sparse solution.

Keywords: computational kinematics, kinematic structure, modular approach
2010 MSC: 00-01, 99-00

1. Introduction

Computational kinematic analysis plays a fundamental role in the study of mechanical systems: first, kinematics is necessary for multibody dynamics; second, kinematics is frequently employed as a first stage in the design process of mechanical systems (dimensional and/or kinematic synthesis); finally, sometimes, the interest of the multibody system (MBS) is purely kinematic (position analysis, range of movement, transmission angle, etc.).

Most of the multibody systems of interest have typically connections (joints) between their bodies, in such a manner that the moving capabilities (the mobility) of the whole MBS is reduced compared to the mobility of the free bodies. The set of coordinates chosen to model the system has to completely (even if not always uniquely) define the position and orientation of all the bodies in the multibody system. Moreover, for kinematics, a number of coordinates equal to the mobility of the system need to be driven in order to be able to calculate the positions and orientations of all the bodies.

1.1. Global and topological approaches

The mathematical model of the MBS can be generated in dependent or independent coordinates. Related to this two possible types of coordinates two different families of methods arise in the kinematic analysis of multibody systems: global and topological. Global methods express the position of each body independently of the rest of bodies of the system, while topological methods express the position of each body by considering the loop (open or closed) to which the body belongs. Thus, topological methods based on independent coordinates are better for open kinematic chains, where the positions, velocities and accelerations of the bodies can be easily expressed analytically by means of these coordinates, but they do not work well in MBS with closed-loops since the equations which define the position

*Principal corresponding author

Email address: msaura.sanchez@upct.es

and orientation of the bodies of the MBS in terms of the independent coordinates are quite complex and, moreover, the solution is normally not unique. In that case, methods based on dependent coordinates are preferred.

The key-point in global formulations is that the set of constraint equations and the rest of matrices needed for the kinematic analysis of the MBS are systematically obtained regardless of the topology of the MBS (open or closed loops), which turns them into a very good candidate for the automatic modeling of multibody systems [1–4]. Also, the constraint equations are really simple when compared to the ones obtained when using relative coordinates and can be programmed and re-used in specific subroutines. An additional advantage for the global approach with natural coordinates is that the size of the problem is smaller than when using reference point coordinates, specially in spatial MBS [5].

One of the main drawbacks of the global formulation is that the number of coordinates, constraint equations and the size of any other matrix involved in the kinematic analysis increases accordingly with the complexity of the problem and the efficient solution of the position, velocity and acceleration problems is a permanent field of research. The use of different linear algebra sparse solvers combined with parallel computing capabilities of new processors, as well as substructuring techniques that divide the MBS into subsystems are currently being studied in the literature. Two examples of the later are the *subsystem segmentation* in which the MBS is divided into smaller subsystems attending to their functionality [6] and the divide and conquer algorithms, allowing the distribution of the computations between several processing cores [7–12].

Topological approaches require a detailed study of the kinematic structure of the MBS to generate the kinematic and dynamic equations which define a MBS. To that end, different methods have been developed: vector-network models, independent open and closed loops identification and modular or component-based decomposition.

Vector-network models have been introduced in 2D MBS [13, 14] and, together with the linear graph theory, efficiently applied to extend the dynamic analysis to a 3D single body [15], and more complex particle systems [16–18] as well as 3D MBS formed by rigid bodies in one closed-loop [19–21] or multiple closure-loops [22–25], modeled with relative and absolute coordinates [26], also in MBS including flexible bodies [27, 28] and in control [29] or optimization problems [30]. Vector-network models represent multibody systems by means of a detailed graph exploited by linear graph theory to generate the equations of motion of multibody systems.

In topological approaches based on the identification of independent open and closed-loops, the topology of the multibody system is represented by a simplified topological graph or the corresponding incidence matrix; linear graph theory is also used, but only from a connectivity point of view. These approaches have been applied in different ways: one of them is to obtain closed-form solutions for the kinematics of single-loop and multiple-loop chains [23, 31]. These closed-form solutions have been successfully applied to obtain and solve symbolic forms of the equations of motion in dynamics of multi-loop mechanisms [25]. An alternative approach are the so called recursive formulations, which make use of an incidence matrix to identify open and closed-loops; they open the closed-loops obtaining a spanned tree whose kinematics can be solved from the base to the leafs by means of kinematic relations between bodies depending on the joints connecting them and loop-closure equations which relate the system coordinates [25, 32–40]. And a third way is to use the topology of the independent open and closed-loops to manipulate the elements in the Jacobian matrix of the constraint equations searching for a reduction in the computational cost of the solution of the complete MBS [41, 42].

Finally, strategies used to formulate and solve the kinematics and dynamics of MBS based on modular decomposition of MBS have also evolved from the basic concept of an Assur group, introduced by Assur at the beginning of the twentieth century, to our days in which the efficiency of this approach has been studied in parallel architectures of high performance computers (HPC) [43]. The topological method based on a modular approach divides a MBS into an ordered set of kinematically determined chains (KDC), known as modules, by applying certain mobility criteria. These modules define the kinematic structure of the multibody system and the kinematics of the whole MBS can be solved by solving each one of the modules in the order defined by its kinematic structure.

A detailed study of the aforesaid topological formulations based on vector-network models and independent open and closed-loops is out of the scope of the present work. Our work will focus in modular decomposition of MBS introducing a systematic methodology to model and solve the kinematics of a general module using two different formulations in natural coordinates and then we will apply this methodology to the kinematic analysis of two scalable MBS which will allow us to compare the efficiency of these two formulations to a global one, also in natural coordinates.

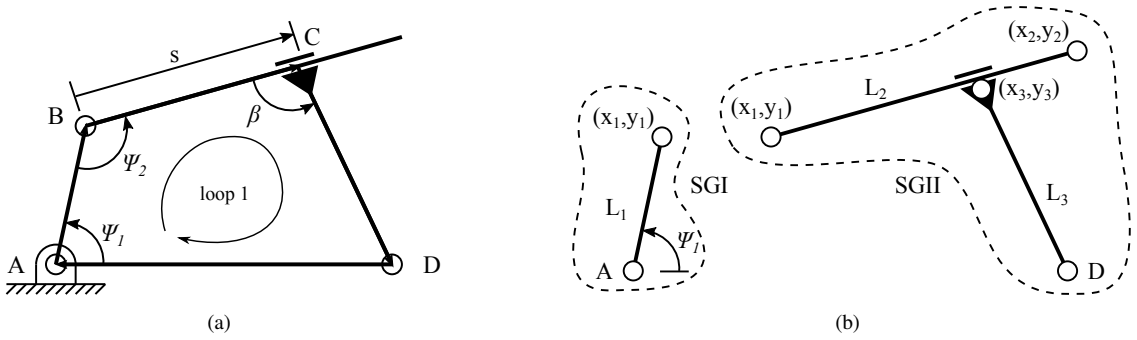

Figure 1: Different topologies of a four-bar linkage: a) One closed-loop; b) Two structural groups: SGI and SGII.

1.2. The modular approach

Some of the global and topological approaches described before for the kinematic and dynamic analysis, need to solve simultaneously the full set of constraint equations of the MBS. In particular, this happens in the subsystem generation, divide and conquer and independent open and closed-loops methods, because the substructures obtained with them do not need to be kinematically determined chains (KDC). Thus the topology of the MBS is not completely exploited in these methods. On the contrary, kinematic substructuring methods make a better job exploiting the topology of the system, since they identify independent KDC which can either be solved in a certain order [22–26] or be used to efficiently organize the elements of the Jacobian matrix of the constraint equations [41, 42]. The kinematic substructuring methods have been developed in two directions: the linear graph algorithms (LGA) identify independent open and closed-loops KDC of reduced size; and the mobility-based algorithms (MBA) in which KDC are obtained by means of algorithms based on mobility criteria [44–51].

In the methods based on linear graph algorithms, the obtained KDC (known as modules) do not always match the number and size of the ones that can be obtained by the MBA methods (also known as modules, structural groups or components) which have the minimum possible size. A very simple example is shown in Fig.1 in which the four-bar linkage shows one single closed-loop in LGA, but it has been divided into two structural groups: SG-I and SG-II of reduced size using MBA methods. As the MBS becomes more complex, the differences between LGA and MBA algorithms are more evident. Moreover, the use of modules in MBA have additional advantages, not only in the analysis of multibody systems but also in dimensional and topological synthesis, which make us focus our interest in this approach. The concept of 'module' as a reference to a KDC is used in both LGA and MBA methods with different topological requirements. In this document the word 'module' will be used as a synonym of structural group (SG): KDC that can not be divided into smaller ones. This concept is the basis of the modular approach.

The modular approach was first introduced by Assur [52] it and has been in permanent development and discussion until our days. In this approach (also known as 'dyad', 'group equations' or 'component' approach) the kinematic structure obtained by means of MBA, informs us about the set of modules (or accordingly: dyads, structural groups or components) in which it can be divided, the sequence in which these modules have been obtained and how they are interconnected. Since all structural groups are KDC, the kinematic analysis of the whole MBS can be achieved by solving each one of them in the specific order defined by its kinematic structure.

Different MBA methods are employed in the literature to obtain the kinematic structure of a MBS and to solve the kinematics of the obtained structural groups. In most of these works the obtained kinematic structure is defined by an ordered set of SG of two types: primary elements (PE) defined as one driving crank or slider that moves with respect to the frame, and Assur groups (AG) of class k defined as 2D kinematic chains with lower kinematic pairs, a number of $N_{\mathrm{m}} = 2k$ bodies and null mobility. A dyad is an AG of class $k = I$ and, by combining how these two bodies can be connected among them and to other bodies of the MBS with revolute (R) or prismatic (P) joints, different types of dyads can be obtained: *RRR, RPR, RRP, PPR, PRP, PPP*. In what follows we will refer as basic multibody systems to those 2D ones which can be divided into one or more PE and a number of dyads, but not AG of larger class.

Modular solutions for basic MBS in which the user must obtain the kinematic structure based on experience have been proposed in [44] and [45]. Both authors offer closed-form solutions for a short list of dyads; they use

trigonometric relationships for the position problem and vector algebra for the velocity and acceleration analysis. In [46] basic MBS are solved with a modular program (the Linkage Analysis Program -LAP-) and the possibility to extend this philosophy to meshing gears, belt/chain drives and cam routines is discussed.

Basic MBS are also studied in [47] but these authors introduce a conceptual algorithm based on mobility criteria to obtain the kinematic structure of 3D MBS searching for single loop determined chains (SLDC) with zero mobility. They also apply previous developments to obtain a closed-form solution for the closure equations for an SLDC. A different MBA for basic MBS is introduced in [48] which exhaustively searches for PE and AG structural groups of a prescribed kind (from a library of nine defined modules) so that the number of PE modules coincides with the mobility of the MBS and all bodies have been assigned to AGs. This author also introduces the concept of floating drivers to solve basic MBS in which the drivers do not actuate over independent coordinates. In those cases the use of the predefined modules is possible by calculating the values of the independent coordinates, their velocities and accelerations in a previous additional stage. An analysis program (CADME) is introduced and its main features compared to other programs based in a similar modular approach: SIMPLA, CRANMEC, N.N. KIDYAN but no evidence of its efficiency or precision is reported. This author assumes without providing any proof a low efficiency of his approach on 3D modules compared to a global approach.

In [49] the kinematics of basic MBS are also solved using a closed-form solution for a short number of dyads in which a linkage can be automatically divided. An optimization method is introduced to transform non-dyad linkages (those that can not be divided into dyads) into a dyad one, so that their kinematics is solvable with accurate results.

The original concept of structural group: primary elements (PE) or Assur group of class k (AG) was extended in [50] to any kinematically determined chain. With this new concept, the kinematic structure of any planar or spatial MBS can be obtained and in [53] we propose a computational method that systematically divides into KDC any planar MBS with different types of kinematic pairs (lower and higher) and any number and distribution of drivers. This method has also successfully been expanded to 3D MBS [54]. However, the kinematics of these new conceptual and more complex 2D and 3D structural groups have not been studied in the literature neither with closed-form nor with iterative solutions.

The modular approach using PE and dyads has also been applied by other authors in the fields of: dynamics of rigid bodies with open loops [55], single-closed-loop rigid body dynamics [56], basic MBS with multiple loops [57, 58] and one-loop flexible MBS [59, 60]. Although no references are made in these works about how to obtain the kinematic substructures of a MBS, except in [60], it is interesting to note that not only in kinematic analysis, but also in dynamics of MBS the matrices associated to specific structural groups can be used to construct the equations of motion of the MBS.

From the literature review it can be concluded that the modular approach is a useful and efficient tool to solve basic MBS by dividing them into simpler KDC whose solution can be previously obtained in closed-form or iterative methods. And not only in kinematic analysis, but also in a broad field of applications in multibody dynamics. However, these solutions have been obtained in all cases in relative coordinates for one-DOF, 2D basic MBS formed by one PE and one dyad whose kinematic solution can be obtained in closed-form due to their simplicity.

The objective in this work is to develop a systematic method which formulates the kinematic solution of any type of KDC regardless of its topology (2D or 3D) number of bodies, type of joints, and number of DOFs, being the use of natural coordinates the best candidate for such task. It would be also of interest to compare the efficiency of the proposed modular approach to the global solution of different 2D and 3D scalable multibody systems; that is, without kinematic substructuring.

In this section, a review of the literature of different topological formulations focused on the modular approach and the motivation of the present study has been established. The rest of the paper is organized as follows: section 2 introduces the global formulation for the kinematic analysis of MBS. This formulation will be used as a basis to develop the kinematic analysis of a module and also to solve the kinematics of the proposed case studies under a global approach. Section 3 introduces the concept of kinematic structure of MBS and the kinematic formulation of a structural group under two approaches: the time derivative and the third-order tensor approach. Section 4 defines two case studies which will be used to evaluate the efficiency of the proposed methods and the algorithms that solve the kinematics of an MBS using both global and modular approaches. Section 5 introduces and discusses the results derived from the implementation of the proposed methods and algorithms, and section 6 gathers the main conclusions obtained from this work and introduces new developments to be accomplished in the future.

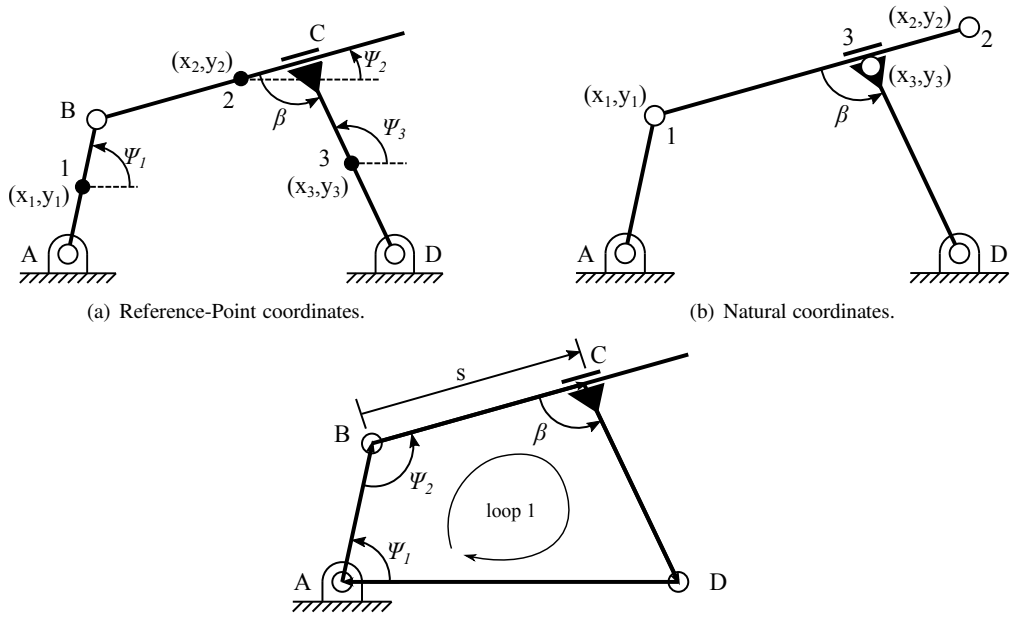

(a) Reference-Point coordinates.

(b) Natural coordinates.

(c) Relative coordinates.

Figure 2: Four bar linkage modeled using different sets of dependent coordinates.

2. Kinematic formulation of MBS: Global approach

It was already mentioned in section 1 that different approaches use different sets of coordinates. In order to illustrate this statement, in Fig.2, different sets global coordinates are used: reference point coordinates Fig.2(a) and natural coordinates Fig.2(b), the ones of interest for this work; moreover, in Fig.2(c), the same system modeled in relative coordinates is represented.

Focusing on the computational kinematic analysis, let's suppose the multibody system (MBS) modeled by means of a set, $\mathbf{q} \in \mathbb{R}^n$, coordinates that completely define the position and orientation of all the bodies in the MBS. If all the N_m movable bodies in the MBS were free to move in space, the total number of independent coordinates of the system would be $n = BN_\mathrm{m}$, where B is a constant: $B = 6$ in spatial MBS and $B = 3$ in planar MBS. However, the bodies in the MBS have typically connections (joints) between them in such a manner that the moving capabilities (the mobility) of the whole system is reduced to f degrees of freedom (DOF).

In a global approach the complete set of n dependent coordinates $\mathbf{q}$ is used to model the MBS. Two methods can be used to solve the kinematic problem: the coordinate partition and the appended driving constraints. In the coordinate partition method, the set of $\mathbf{q}$ coordinates is partitioned into a subset of f independent coordinates $\mathbf{q}^\mathrm{i}$ and a subset of m dependent ones $\mathbf{q}^\mathrm{d}$. Independent coordinates and their time derivatives are evaluated before the dependent ones, at any instant of time, by means of a set of driving constraints $\mathbf{\Phi}^\mathrm{D}$ which relate the independent coordinates with the time variable. Then, the dependent coordinates are calculated by solving the corresponding constraint equations $\mathbf{\Phi}(\mathbf{q}, t)$.

In the appended driving constraints method, the values of the independent coordinates are calculated together with the values of the dependent ones by appending the driving constraints $\mathbf{\Phi}^\mathrm{D}(\mathbf{q}, t)$ to the set of rigid-body and kinematic constraint equations $\mathbf{\Phi}(\mathbf{q}, t)$:

$$\begin{aligned} \mathbf{\Phi}(\mathbf{q}, t) &= \mathbf{0} \\ \mathbf{\Phi}^\mathrm{D}(\mathbf{q}^\mathrm{i}, t) &= \mathbf{0} \end{aligned} \tag{1}$$

It will be assumed hereafter a compact form of the set of constraints $\mathbf{\Phi}(\mathbf{q}, t)$ which contains all the kinematic and the driving (rheonomous) constraints. Then, if the coordinate partition method is used, it is supposed that, at any instant of time, the independent coordinates will be evaluated before the dependents by means of the $\mathbf{\Phi}^\mathrm{D}$ driving

constraints. Otherwise, both the dependent and the independent coordinates will be solved simultaneously by means of Eq.(1).

Natural coordinates, the ones of interest for the present work, are cartesian coordinates of body-fixed entities (points and vectors) used to sistematically model multibody systems. In the case shown in Fig.2(b) this type of coordinates are used to model the four-bar linkage and for each one of the N_m movable bodies a scalar condition of rigid body $\mathbf{\Phi}^\mathrm{RB}$ has to be imposed:

$$\mathbf{\Phi}^\mathrm{RB} = \mathbf{r}_{ij}^\mathrm{T}\mathbf{r}_{ij} - L_{ij}^2 = 0 \tag{2}$$

where i and j are two points belonging to the considered rigid body and L_{ij} is the constant distance between them. In addition, for some kinematic joints, additional constraint equations must be also appended, rising the number of scalar constraint equations up to five. If one driving constraint is defined for the independent coordinate (i.e. $x_1 - 5t = 0$), then the kinematics of the system has been completely defined or *kinematically determined*. For more details on modeling with natural coordinates, see [61].

Once the MBS has been modeled using the selected type of coordinates, all these coordinates will be related between them by means of the corresponding set of constraint equations:

$$\mathbf{\Phi}(\mathbf{q}, t) = \mathbf{0} \tag{3}$$

For the mechanism shown in Fig.2.b the dependent coordinates are $\mathbf{q} = [x_1\ y_1\ x_2\ y_2\ x_3\ y_3]$, and the corresponding constraint equations:

$$\mathbf{\Phi} = \begin{bmatrix} \mathbf{r}_{1\mathrm{A}}^\mathrm{T}\mathbf{r}_{1\mathrm{A}} - L_{1\mathrm{A}}^2 \\ \mathbf{r}_{21}^\mathrm{T}\mathbf{r}_{21} - L_{21}^2 \\ \mathbf{r}_{3\mathrm{D}}^\mathrm{T}\mathbf{r}_{3\mathrm{D}} - L_{3\mathrm{D}}^2 \\ \mathbf{r}_{21}\mathbf{r}_{3\mathrm{D}} - L_{21}L_{3\mathrm{D}}\cos\beta \\ \mathbf{r}_{21} \times \mathbf{r}_{31} \end{bmatrix} = [\mathbf{0}]_{6\times 1} \tag{4}$$

Eqs.(4) form a set of constraint equations that allows us to calculate five coordinates from $\mathbf{q}$ when the value of the remaining one is known.

In order to solve the position problem, at each time step the f independent coordinates and their first and second time derivatives: $\mathbf{q}^\mathrm{i}$, $\dot{\mathbf{q}}^\mathrm{i}$, $\ddot{\mathbf{q}}^\mathrm{i}$ are evaluated, and then, the m dependent coordinates $\mathbf{q}^\mathrm{d}$ can be calculated by means of the Newton-Raphson numerical iterative method:

$$\left(\mathbf{\Phi}_{\mathbf{q}^\mathrm{d}}\right)_{k-1}\left(\mathbf{q}_k^\mathrm{d} - \mathbf{q}_{k-1}^\mathrm{d}\right) = -\mathbf{\Phi}_{k-1} \tag{5}$$

where $\mathbf{\Phi}_{\mathbf{q}^\mathrm{d}}$ represents the Jacobian matrix of the constraint equations with respect to the m dependent coordinates. The elements of the Jacobian matrix can be systematically obtained and appended for each kind of constraint equation; For example, for the constraint equations $\mathbf{\Phi}^\mathrm{RB}$ in Eq.(2), one obtains:

$$\mathbf{\Phi}_{\mathbf{q}^\mathrm{d}}^\mathrm{RB} = \left[\frac{\mathrm{d}\mathbf{\Phi}^\mathrm{RB}}{\mathrm{d}\mathbf{q}^\mathrm{d}}\right]_{1\times m} \tag{6}$$

Once the position problem is solved, at each time step, the dependent velocities can be obtained by deriving the constraint equations at position level Eq.(3) with respect to time. Then, the resulting system of linear equations for velocities can be solved by using again the coordinate partition method:

$$\dot{\mathbf{\Phi}}(\mathbf{q}, t) = \mathbf{0} \tag{7a}$$

$$\mathbf{\Phi}_{\mathbf{q}^\mathrm{d}}\dot{\mathbf{q}}^\mathrm{d} + \mathbf{\Phi}_{\mathbf{q}^\mathrm{i}}\dot{\mathbf{q}}^\mathrm{i} = -\mathbf{\Phi}_t \tag{7b}$$

$$\mathbf{\Phi}_{\mathbf{q}^\mathrm{d}}\dot{\mathbf{q}}^\mathrm{d} = -\left[\mathbf{\Phi}_{\mathbf{q}^\mathrm{i}}\dot{\mathbf{q}}^\mathrm{i} + \mathbf{\Phi}_t\right] \tag{7c}$$

In Eq.(7c), $\mathbf{\Phi}_{\mathbf{q}^{\mathrm{i}}}$ and $\mathbf{\Phi}_t$ represent the Jacobian matrix of the constraint equations with respect to the f independent $\mathbf{q}^{\mathrm{i}}$ coordinates and the time t respectively. For the constraint equation Eq.(2), one obtains:

$$\mathbf{\Phi}^{\mathrm{RB}}_{\mathbf{q}^{\mathrm{i}}} = \left[\frac{\mathrm{d}\mathbf{\Phi}^{\mathrm{RB}}}{\mathrm{d}\mathbf{q}^{\mathrm{i}}}\right]_{1\times f} \tag{8}$$

Finally, the acceleration problem is solved by deriving again the constraint equations at velocity level Eq.(7a), with respect to time:

$$\ddot{\mathbf{\Phi}}(\mathbf{q}, t) = \mathbf{0} \tag{9}$$

By means of the coordinate partition method, the dependent accelerations can be expressed in terms of all the velocities $\dot{\mathbf{q}}$ and the independent accelerations $\ddot{\mathbf{q}}^{\mathrm{i}}$ as:

$$\mathbf{\Phi}_{\mathbf{q}^{\mathrm{d}}}\ddot{\mathbf{q}}^{\mathrm{d}} + \mathbf{\Phi}_{\mathbf{q}^{\mathrm{i}}}\ddot{\mathbf{q}}^{\mathrm{i}} + \dot{\mathbf{\Phi}}_{\mathbf{q}}\dot{\mathbf{q}} + \dot{\mathbf{\Phi}}_t = \mathbf{0} \tag{10a}$$

$$\mathbf{\Phi}_{\mathbf{q}^{\mathrm{d}}}\ddot{\mathbf{q}}^{\mathrm{d}} = -(\mathbf{\Phi}_{\mathbf{q}^{\mathrm{i}}}\ddot{\mathbf{q}}^{\mathrm{i}} + \dot{\mathbf{\Phi}}_{\mathbf{q}}\dot{\mathbf{q}} + \dot{\mathbf{\Phi}}_t) \tag{10b}$$

In Eq.(10b), the column matrix $\dot{\mathbf{\Phi}}_{\mathbf{q}}\dot{\mathbf{q}}$ is obtained as a matrix vector product, where the matrix $\dot{\mathbf{\Phi}}_{\mathbf{q}}$ is obtained as the time derivative of the Jacobian matrix of the constraint equations differentiated with respect to the complete set $\mathbf{q}$ of coordinates, and their velocities $\dot{\mathbf{q}}$ are known from the velocity stage of the analysis.

3. Kinematic formulation of MBS: Modular approach

To solve the kinematics of a multibody system with a modular approach, the first step consists of obtaining the kinematic structure of the MBS, which informs about how many SG compose the MBS and the specific order in which these SG have to be analysed. Then, applying the method of group equations to each one of the SG in the specific order they have been obtained, the kinematic analysis of the whole MBS is achieved.

3.1. Kinematically determined chains (KDC)

From the theory of mechanism and machines, it is known that the mobility L_{c} of an holonomous kinematic chain defines its number of degrees of freedom (DOF), which can be calculated, in general, as:

$$L_{\mathrm{c}} = BN_{\mathrm{m}} - \sum_{k=1}^{B-1} e_k P_k \tag{11}$$

where: B has already been defined, N_{m} represents the number of movable bodies in the kinematic chain, P_k is the number of kinematic pairs of grade k (DOF allowed between two connected bodies), and e_k is the DOF removed by a kinematic pair of grade k ($e_k = B - k$). In P_k both internal and external kinematic pairs must be considered. Internal kinematic pairs are those formed between bodies from the same kinematic chain, whereas external kinematic pairs are those formed between two bodies from different kinematic chains. Equation Eq.(11) is valid for most kinematic chains, except for those in which well-known special topological or kinematic conditions appear (i.e. pure rolling). We will restrict ourselves to the study of holonomic kinematic chains in which Eq.(11) apply.

The mobility f of a MBS is calculated using Eq.(11) as if it were formed by an unique kinematic chain. Then, if the set of independent coordinates $\mathbf{q}^{\mathrm{i}} \in \mathbb{R}^f$ are defined by means of driving constraints, the MBS is kinematically determined, as defined in section 2. These independent coordinates are also known by different authors as driven coordinates or input motions of the MBS.

In the modular approach, MBS are studied as a combination of kinematically determined chains (KDC): kinematic chains that have their L_{c} DOFs defined by a subset of $n_{\mathrm{c}} = L_{\mathrm{c}}$ out of the $\mathbf{q}^{\mathrm{i}}$ driven coordinates. As an example, Fig.1(a) shows a four-bar MBS of mobility $f = 1$ and, in order to be kinematically determined, one independent coordinate must be driven (i.e. $\mathbf{q}^{\mathrm{i}} = \Psi_1$). The same driven coordinate is considered in Fig.1(b) but, in this figure, the MBS is composed of two kinematic chains: SG-I and SG-II whose mobility are $L_{\mathrm{cSG-I}} = 1$ and $L_{\mathrm{cSG-II}} = 0$ respectively. The first kinematic chain SG-I is a KDC as one driven coordinate, Ψ_1, from $\mathbf{q}^{\mathrm{i}}$ is considered, and $n_{\mathrm{cSG-I}} = L_{\mathrm{cSG-I}}$. The second kinematic chain SG-II is also a KDC as zero driven coordinates from $\mathbf{q}^{\mathrm{i}}$ are considered and $n_{\mathrm{cSG-II}} = L_{\mathrm{cSG-II}}$. Dividing a MBS into an ordered set of KDCs is the main objective of the structural analysis theory and, as the result of such process, the kinematic structure of a MBS is obtained.

3.2. Kinematic structure of a multibody system

The theory of structural analysis defines a structural group as a KDC ($n_c = L_c$). If a structural group (SG) has neither excessive constrains, nor additional DOF due to special geometric considerations, it is defined as a *normal* SG [50]. Furthermore, one normal SG which cannot be split into other normal SGs of smaller number of bodies are denominated *simple* SG. Then, the kinematic structure of a MBS is defined as an ordered set of simple SG in which a MBS can be divided; this division is not unique and depends on the topology of the MBS and the selected driven coordinates of the MBS.

Multibody systems can be both divided into or built from an ordered set of simple SG. By combining Eq.(11) and the condition of simple SG ($n_c = L_c$), we can obtain the generation principle of mechanisms (Eq.(12)), which is the necessary condition for any kinematic chain to be a simple SG.

$$S_c - n_c = B(P - N_m) \tag{12}$$

where S_c is defined as the number of DOF allowed by the P kinematic pairs formed by the N_m mobile bodies of the kinematic chain, and n_c is the number of the input motions (out of $\mathbf{q}^i$) that are present in the kinematic chain. In order to apply Eq.(12) correctly, the parameter S_c is calculated as:

$$S_c = \sum_{k=1}^{B-1} kP_k \tag{13}$$

and it must be considered that, in Eq.(13), P_k refers to all internal kinematic pairs and, from the external ones, only those with a directed edge in the structural graph, as it will be explained later.

The generation principle of mechanisms (Eq.(12)) can be applied to obtain the kinematic structure of a MBS by means of graph-analytical [50, 53] or computational [53] methods. Due to its simplicity, the graph-analytical method is introduced here and applied, as an example, to the four-bar linkage shown in Fig.3(a). For a computational algorithm that automatically obtains the kinematic structure of planar MBS, see [53].

In the graph-analytical method, the *structural graph* represents the topology of the MBS by means of graph theory elements. There are many forms in which the topology of a MBS can be represented by a structural graph, and the most frequently used in the literature are discussed in [53]. For the purposes of an efficient structural analysis, we use the one shown in Fig.3(b): vertices (1 to 4) correspond to bodies, and bodies that form a kinematic pair are connected by a number of edges (thin lines) equal to the degree k of the kinematic pair. Moreover, a number of thin lines equal to the driven coordinates in a kinematic pair become bold lines, which are known as root edges. In the example, lower kinematic pairs ($k = 1$) connect bodies: $(1-2,\ 2-3,\ 3-4,\ 1-4)$, and $(1-2)$ is a root edge because the relative motion it represents (θ_1) is a driven one.

The structural analysis starts by removing the frame from the structural graph. Since the frame is not allowed to move, all the relative motions between the frame and the bodies attached to it must be considered as DOF assigned to the corresponding bodies (2 and 4) by means of directed edges, as shown in Fig.3(c). Any body that receives DOF, from the frame or from other bodies in a later stage of the structural analysis, becomes a candidate to form a structural group. If one candidate satisfies Eq.(12) then it is a SG.

By considering Eq.(13) and the fact that each thin and bold line identifies one DOF in the structural graph we rewrite Eq.(12) as:

$$L_{th} = B(P - N_m) \tag{14}$$

so that if the left hand side of Eq.(14) equals the right hand side, the kinematic chain is a simple SG. Recall that, in Eq.(14), P is the number of kinematic pairs in the kinematic chain: internal kinematic pairs and, from the external ones, only those with a directed edge and L_{th} is the number of thin lines that corresponds to these P kinematic pairs.

With the considerations made above, and with the support of the structural graph, the kinematic structure of the MBS is obtained in a very simple manner, as depicted in Figs. 3(c) to 3(f), following four basic steps:

Step 1: Frame (body 1) isolation and DOF assignment (Fig.3(c)). The DOF of the kinematic pairs between movable bodies (2, 4) and the frame (1) are assigned to the former ones. These bodies become *candidates* to be a SG.

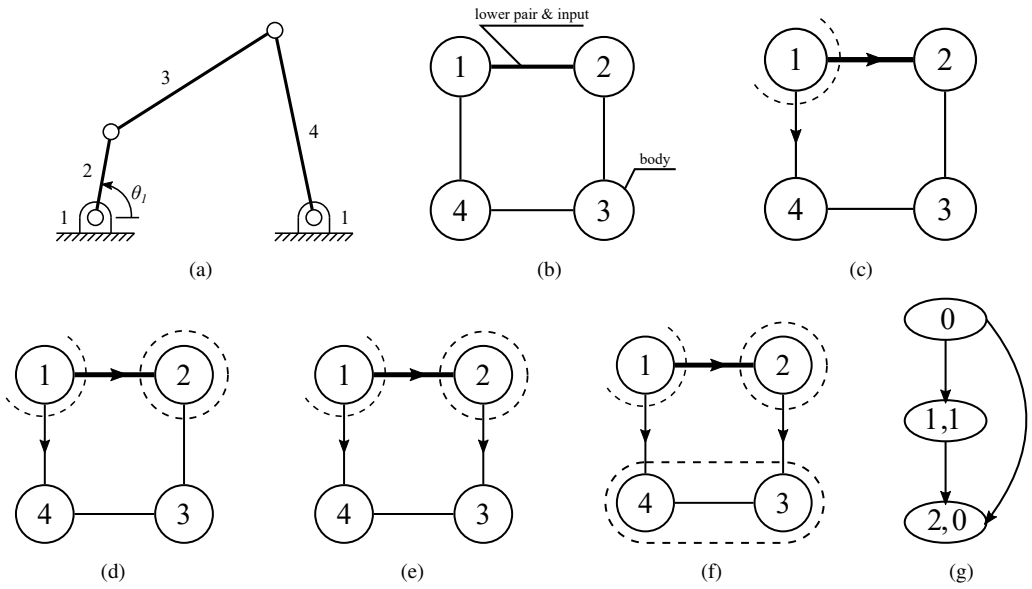

Figure 3: Four-bar linkage. a) Kinematic graph. b) Structural graph. c) to f) Steps to perform structural analysis through its structural graph. g) Structural diagram.

Step 2: Search for a SG from shorter to larger length. Each one of the candidates is a kinematic chain that has to satisfy Eq.(14) in order to be a SG. In Fig.3(c), the candidate of the kinematic chain $\{4\}$ is a single body ($N_{\mathrm{m}} = 1$) that participates in one directed external kinematic pair $1-4$ and zero internal kinematic pairs, so $P = 1$. Note that the edge $3-4$ is neither an internal pair nor an external directed one, so $L_{\mathrm{th}} = 1$ and Eq.(14) is not fulfilled as $1 \neq 3(1-1)$ and $\{4\}$ does not form SG. Then, candidate 2 is studied (Fig.3(d)). This kinematic chain $\{2\}$ only participates in one directed external pair $1-2$ which is a root edge, then: $N_{\mathrm{m}} = 1$, $P = 1$ and $L_{\mathrm{th}} = 0$. Thus, for this body it can be found that Eq.(14) is satisfied and this body is a simple SG.

Step 3: Reassign DOF. If a kinematic chain forms a SG, the DOF of its non directed external pairs are assigned to the bodies of the corresponding external pair. In the example, body 2 is a SG and assigns the DOF $(2-3)$ to body 3, which now becomes a new *candidate* (Fig.3(e)). There are no more DOFs assignments.

Step 4: Turn to Step 2 until the complete kinematic structure of the MBS is obtained. Bodies 3 and 4 are *candidates*. Kinematic chains of only one candidate $\{3\}$ or $\{4\}$ does not satisfy Eq.(14) as $L_{\mathrm{th}} = 1$. Then, larger chains must be considered. Starting from a candidate, e.g. body 3, the chain is expanded by selecting another body (candidate or not) that forms a kinematic pair with the selected candidate. Chain $\{3, 4\}$, whose parameters are: $L_{\mathrm{th}} = 3$; $N_{\mathrm{m}} = 2$; $P = 3$ satisfies Eq.(14) and therefore it is a simple SG (Fig.3(f)).

Structural diagram. The kinematic structure of a mechanism is graphically represented by its *structural diagram* Fig.3(g). It is composed by as many circles as SG define the kinematic structure plus one, corresponding to the frame, which is identified with the number 0 in it. The two parameters inside each circle are $(N_{\mathrm{m}}, n_{\mathrm{c}})$. An arrow joins two circles if any of their bodies form an external kinematic pair, and it is directed in the same direction as the DOF assigned during the structural analysis, showing the order in which the SG have been obtained and dictating the sequence in which their kinematics have to be solved. In the four-bar linkage, the frame assigns DOF to bodies 2 and 4, and body 2 assigns DOF to body 3. This means that to solve the kinematics of the whole MBS, first the kinematics of SG $\{2\}$ must be solved and then, the kinematics of SG $\{3, 4\}$.

Any kinematically determined MBS can be divided into SG regardless its topology and mobility. Different cases have been studied for 2D MBS with lower and higher kinematic pairs in [53] and an extension of this computational method to 3D MBS will be presented in a separated paper. Moreover, the kinematic structure of a MBS which satisfies Eq.(11) is unique for a given set of independent coordinates $\mathbf{q}^{\mathrm{i}}$.

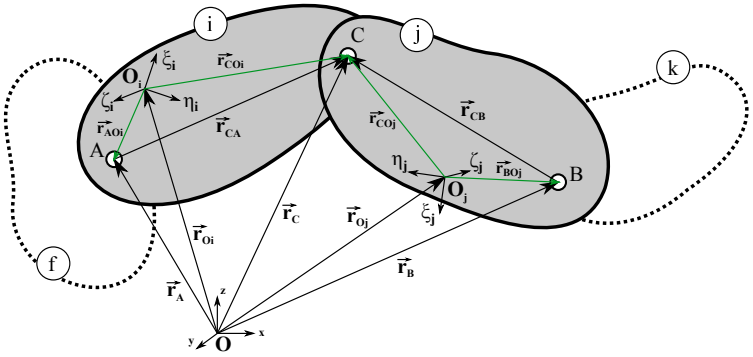

Figure 4: A planar SG formed by two bodies $\{i, j\}$, with one internal kinematic pair and two external ones: $\{f, i\}, \{j, k\}$. Independent group coordinates: $\vec{r}_A$ and $\vec{r}_B$ are known from previous SG and dependent group coordinates: $\vec{r}_C$ are to be determined.

3.3. Kinematic formulations of a structural group

The kinematic analysis of a MBS can be carried out by solving, at each calculation step, the kinematics of each one of its SG, in the specific order defined by its kinematic structure. One of the main advantages of the topological formulation based on group equations is that the kinematic analysis of any SG can be programmed in specific separated (reusable) subroutines, whose writing can be standardized following a few steps as introduced in this section. The kinematic analysis of any SG deals with the solution of the position, velocity and acceleration problems of the corresponding subsystem. In this section, the kinematic analysis of a general SG (Fig.4) is described. Then, two different approaches for the solution of the acceleration problem are introduced: the first one uses the time derivative of the Jacobian matrix of the group equations and, in the second one, the same Jacobian matrix is derived with respect to the vector of independent coordinates of the SG.

A. Position problem. Fig.4 shows a planar SG formed by two bodies $\{i, j\}$ linked at point C (internal kinematic pair), which are linked to other two different bodies f and k, forming two external kinematic pairs $\{f, i\}$ and $\{j, k\}$. This structural group is known as 3R, because of its three revolute kinematic pairs. Since the kinematic chain $\{i, j\}$ is a SG, bodies f and k must belong to other SG previously obtained or to the frame. Without loss of generality, this SG will be used to illustrate the kinematic analysis based on group equations.

The kinematics of any SG can be solved if the appropriate set of group coordinates $\mathbf{q}_{\mathrm{SG}}$ are selected to modelize the SG and the corresponding constraint equations $\mathbf{\Phi}$ defined.

Identify the group coordinates and parameters. A local coordinate system $\{\eta_i, \xi_i, \zeta_i\}, \{\eta_j, \xi_j, \zeta_j\}$ is attached to each body in the SG and the appropiate set of group coordinates that defines the kinematic chain is selected. In this paper, only natural coordinates will be considered, although other types of coordinates: reference point or relative coordinates can be employed.

When modeling a structural group in natural coordinates, points and vectors must be considered so that all their bodies can be defined as rigid and all the degrees of freedom constrained by their joints are considered. The cartesian coordinates of the entities that connects the bodies of the structural group to the frame or to bodies of already solved structural groups will enter in the subset of independent group coordinates $\mathbf{h}$, and therefore their values are known. On the other hand, the cartesian coordinates used to define the rigid-body conditions or the constrained degrees of freedom of the internal kinematic pairs of the structural group, as well as entities needed to solve other SGs in the kinematic structure, will enter in the subset of dependent group coordinates $\boldsymbol{\varphi}$. Both subsets of coordinates form the set of group coordinates $\mathbf{q}_{\mathrm{SG}}$ which are related by means of $\mathbf{\Phi}_{\mathrm{SG}}$, the constraint equations obtained from rigid-body and kinematic-pair conditions. Let r and s be the number of dependent and independent group coordinates respectively and p the number of constraint equations of the structural group and lets see two examples of these sets of group coordinates.

In the planar structural group of Fig.4 these sets of coordinates are: $\boldsymbol{\varphi} = [x_C, y_C]$ and $\mathbf{h} = [x_A, y_A, x_B, y_B]$ respectively, and if the values of the $\mathbf{h}$ coordinates are known, then the values of the dependent ones can be calculated from the rigid-body conditions of bodies i and j.

For the mechanism shown in Fig.2.b, we have two structural groups. The first one has: $\mathbf{q}_{\mathrm{SG}} = [x_1\ y_1]$ and we can consider: $\mathbf{h} = x_1$ known, and $\boldsymbol{\varphi} = y_1$. The rigid-body constraint equation for this SG:

$$\boldsymbol{\Phi} = \mathbf{r}_{1\mathrm{A}}^{\mathrm{T}}\mathbf{r}_{1\mathrm{A}} - L_{1\mathrm{A}}^2 = 0 \tag{15}$$

allows us to determine the value of the dependent coordinate.

For the second structural group: $\mathbf{q}_{\mathrm{SG}} = [x_1\ y_1\ x_2\ y_2\ x_3\ y_3]$; we must consider: $\mathbf{h} = [x_1\ y_1]$ as independent (known) and $\boldsymbol{\varphi} = [x_2\ y_2\ x_3\ y_3]$ and the constraint equations are obtained and appended due to rigid-body and kinematic pair conditions:

$$\boldsymbol{\Phi} = \begin{bmatrix} \mathbf{r}_{21}^{\mathrm{T}}\mathbf{r}_{21} - L_{21}^2 \\ \mathbf{r}_{3D}^{\mathrm{T}}\mathbf{r}_{3\mathrm{D}} - L_{3\mathrm{D}}^2 \\ \mathbf{r}_{21}\mathbf{r}_{3\mathrm{D}} - L_{21}L_{3\mathrm{D}}\cos\beta \\ \mathbf{r}_{21} \times \mathbf{r}_{31} \end{bmatrix} = [\mathbf{0}]_{5\times 1} \tag{16}$$

which is a redundant set of constraint equations that can be solved as introduced in the following sections.

Position problem for the SG. To solve the position problem of any SG, the corresponding group equations that relate the dependent and independent group coordinates must be defined.

$$\boldsymbol{\Phi}(\boldsymbol{\varphi}, \mathbf{h}, t) = \mathbf{0} \tag{17}$$

For the structural group in (Fig.4), only rigid body constraints apply:

$$\boldsymbol{\Phi}(\boldsymbol{\varphi}, \mathbf{h}, t) = \begin{bmatrix} \mathbf{r}_{\mathrm{CA}}^{\mathrm{T}}\mathbf{r}_{\mathrm{CA}} - L_{\mathrm{AC}}^2 \\ \mathbf{r}_{\mathrm{CB}}^{\mathrm{T}}\mathbf{r}_{\mathrm{CB}} - L_{\mathrm{BC}}^2 \end{bmatrix} = \mathbf{0} \tag{18}$$

Then, the Newton-Raphson iterative method is applied to obtain the values of the dependent group coordinates:

$$\left(\boldsymbol{\Phi}_{\boldsymbol{\varphi}}\right)_{k-1}(\boldsymbol{\varphi}_k - \boldsymbol{\varphi}_{k-1}) = -\boldsymbol{\Phi}_{k-1} \tag{19a}$$

where $\boldsymbol{\Phi}_{\boldsymbol{\varphi}}$ represents the Jacobian matrix of the constraint equations with respect to the dependent coordinates, whose terms, in SG with a reduced number of bodies, can be obtained in symbolic form (Eq.(19b)).

In the example of the 3R SG from Fig.4, this Jacobian matrix can be obtained in symbolic form as:

$$\boldsymbol{\Phi}_{\boldsymbol{\varphi}} = \begin{bmatrix} 2\,(x_C - x_A) & 2\,(y_C - y_A) \\ 2\,(x_C - x_B) & 2\,(y_C - y_B) \end{bmatrix} \tag{19b}$$

In order to reduce the computation time, and depending on the size of the matrices involved in the kinematic analysis of the SG, the solution of the position problem might be achieved by selecting the most appropriate method: LU, QR decomposition, or even a direct computation of the inverse of the Jacobian matrix $\boldsymbol{\Phi}_{\boldsymbol{\varphi}}^{-1}$. For the 3R SG considered in Eq.(19b), the inverse of the Jacobian matrix can be easily obtained and used directly in the position problem although, in most cases, this solution is not the most efficient.

$$\left(\boldsymbol{\Phi}_{\boldsymbol{\varphi}}\right)^{-1} = \frac{1}{\chi}\begin{bmatrix} (y_C - y_B) & -(y_C - y_A) \\ -(x_C - x_B) & (x_C - x_A) \end{bmatrix} \tag{20a}$$

$$\chi = 2(x_A y_B - x_B y_A - x_A y_C + x_C y_A + x_B y_C - x_C y_B) \tag{20b}$$

However, in the most general case, the number of constraint equations of the structural group p exceeds the number of dependent coordinates r; the Jacobian matrix $\boldsymbol{\Phi}_{\boldsymbol{\varphi}}$ is not square and can not be inverted. Among the different solutions proposed in the literature, the least square method described in [61] is used in this work. In such cases, the position problem is formulated as:

$$\left(\boldsymbol{\Phi}_{\boldsymbol{\varphi}}^{\mathrm{T}}\boldsymbol{\Phi}_{\boldsymbol{\varphi}}\right)_{k-1}(\boldsymbol{\varphi}_k - \boldsymbol{\varphi}_{k-1}) = -\left(\boldsymbol{\Phi}_{\boldsymbol{\varphi}}^{\mathrm{T}}\boldsymbol{\Phi}\right)_{k-1} \tag{21}$$

where $\boldsymbol{\Phi}_{\boldsymbol{\varphi}}^{\mathrm{T}}$ is the transpose of matrix $\boldsymbol{\Phi}_{\boldsymbol{\varphi}}$.

B. Velocity problem. The velocity problem can be formulated by deriving the constraint equations Eq.(17) with respect to time and solving the resulting system of linear equations for the dependent velocities.

$$\dot{\mathbf{\Phi}}(\boldsymbol{\varphi}, \mathbf{h}, t) = \mathbf{0} \tag{22a}$$

$$\mathbf{\Phi}_{\boldsymbol{\varphi}}\dot{\boldsymbol{\varphi}} + \mathbf{\Phi}_{\mathbf{h}}\dot{\mathbf{h}} + \mathbf{\Phi}_t = \mathbf{0} \tag{22b}$$

$$\mathbf{\Phi}_{\boldsymbol{\varphi}}\dot{\boldsymbol{\varphi}} = -\left[\mathbf{\Phi}_{\mathbf{h}}\dot{\mathbf{h}} + \mathbf{\Phi}_t\right] \tag{22c}$$

where the independent group velocities $\dot{\mathbf{h}}$, the Jacobian matrix with respect the independent group coordinates $\mathbf{\Phi}_{\mathbf{h}}$ and the partial derivative of the constraint equations with respect to time $\mathbf{\Phi}_t$ are known. In the general case, in which $p > r$, the velocity problem shown in Eq.(22c) has to be reformulated as:

$$\mathbf{\Phi}_{\boldsymbol{\varphi}}^{\mathrm{T}}\mathbf{\Phi}_{\boldsymbol{\varphi}}\dot{\boldsymbol{\varphi}} = -\mathbf{\Phi}_{\boldsymbol{\varphi}}^{\mathrm{T}}\left[\mathbf{\Phi}_{\mathbf{h}}\dot{\mathbf{h}} + \mathbf{\Phi}_t\right] \tag{23}$$

Then, dependent velocities $\dot{\boldsymbol{\varphi}}$ are obtained by using the most appropiate method, depending on the size of the matrices involved in the analysis. For the 3R structural group, a symbolic form of these Jacobians matrices can be obtained.

$$\mathbf{\Phi}_{\mathbf{h}} = \begin{bmatrix} -2\,(x_C - x_A) & -2\,(y_C - y_A) & 0 & 0 \\ 0 & 0 & -2\,(x_C - x_B) & -2\,(y_C - y_B) \end{bmatrix} \tag{24a}$$

$$\mathbf{\Phi}_t = \begin{bmatrix} 0 \\ 0 \end{bmatrix} \tag{24b}$$

Velocity coefficients matrix. Eqs.(22c) and (23) show that the dependent velocities $\dot{\boldsymbol{\varphi}}$ are obtained as the sum of two terms: the first one expresses the dependent velocities as a linear combination of the independent ones $\dot{\mathbf{h}}$ and the second term considers the dependency of the constraint equations with respect to the time variable.

Lets consider the case in which $p = r$ and lets define matrix $\mathbf{K}_{\boldsymbol{\varphi}\mathbf{h}}$, matrix $\mathbf{S}$ and column matrix $\mathbf{b}$ as:

$$\mathbf{\Phi}_{\boldsymbol{\varphi}}\mathbf{K}_{\boldsymbol{\varphi}\mathbf{h}} = -\mathbf{\Phi}_{\mathbf{h}} \tag{25a}$$

$$\mathbf{\Phi}_{\boldsymbol{\varphi}}\mathbf{S} = \mathbf{I} \tag{25b}$$

$$\mathbf{b} = -\mathbf{\Phi}_t \tag{25c}$$

where matrix $\mathbf{K}_{\boldsymbol{\varphi}\mathbf{h}}$ is known as the velocity coefficients matrix and $\mathbf{I} \in \mathbb{R}^{r\times r}$ is the identity matrix, then these dependencies become more clear:

$$\dot{\boldsymbol{\varphi}} = \mathbf{K}_{\boldsymbol{\varphi}\mathbf{h}}\dot{\mathbf{h}} + \mathbf{S}\mathbf{b} \tag{26}$$

In very simple SG, not only the Jacobian matrices $\mathbf{\Phi}_{\boldsymbol{\varphi}}$, $\mathbf{\Phi}_{\mathbf{h}}$ and $\mathbf{\Phi}_t$, but also the velocity coefficients $\mathbf{K}_{\boldsymbol{\varphi}\mathbf{h}}$, and the column matrix $\mathbf{S}\mathbf{b}$ can be obtained in symbolic form. In the example of the 3R SG (where χ is the same as Eq.(20b)):

$$\mathbf{K}_{\boldsymbol{\varphi}\mathbf{h}} = \frac{1}{\chi}\begin{bmatrix} 2(x_A - x_C)(y_B - y_C) & 2(y_A - y_C)(y_B - y_C) & -2(x_B - x_C)(y_A - y_C) & -2(y_B - y_C)(y_A - y_C) \\ -2(x_A - x_C)(x_B - x_C) & -2(y_A - y_C)(x_B - x_C) & 2(x_B - x_C)(x_A - x_C) & 2(y_B - y_C)(x_A - x_C) \end{bmatrix} \tag{27}$$

However, in complex MBS the velocity coefficients matrix can not be obtained in a symbolic form, and the solution of Eq.(26) is less efficient than the system shown in Eq.(22c). In order to solve Eq.(26): first, each column in the $\mathbf{K}_{\boldsymbol{\varphi}\mathbf{h}}$ matrix has to be obtained by solving Eq.(25a) s times and then, Eq.(26) has to be solved to obtain the dependent velocities.

In the general case, in which $p > r$, Eq.(23) apply, but the solution given by Eq.(26) might be used by redefining matrices $\mathbf{K}_{\boldsymbol{\varphi}\mathbf{h}}$, matrix $\mathbf{S}$ and column matrix $\mathbf{b}$ as:

$$\boldsymbol{\Phi}_{\boldsymbol{\varphi}}^{\mathrm{T}}\boldsymbol{\Phi}_{\boldsymbol{\varphi}}\mathbf{K}_{\boldsymbol{\varphi}\mathbf{h}} = -\boldsymbol{\Phi}_{\boldsymbol{\varphi}}^{\mathrm{T}}\boldsymbol{\Phi}_{\mathbf{h}} \tag{28a}$$

$$\left(\boldsymbol{\Phi}_{\boldsymbol{\varphi}}^{\mathrm{T}}\boldsymbol{\Phi}_{\boldsymbol{\varphi}}\right)\mathbf{S} = \mathbf{I} \tag{28b}$$

$$\mathbf{b} = -\boldsymbol{\Phi}_{\boldsymbol{\varphi}}^{\mathrm{T}}\boldsymbol{\Phi}_{t} \tag{28c}$$

The velocity coefficients matrix is required to solve the acceleration problem as a part of the third-order tensor approach presented in the following section.

C. Acceleration problem. To solve the acceleration problem for the dependent group coordinates, two approaches are considered in this study: the time derivative approach and the third-order tensor approach.

Option 1: Time derivative approach. The acceleration problem is solved by deriving the constraint equations at a velocity level Eq.(22c) with respect to time:

$$\ddot{\boldsymbol{\Phi}}(\boldsymbol{\varphi}, \mathbf{h}, t) = \mathbf{0} \tag{29}$$

Lets define the column matrix $\mathbf{q}_{\mathrm{G}}$ as the group coordinates matrix, which contains all the $\boldsymbol{\varphi}$ dependent and $\mathbf{h}$ independent group coordinates, and $\dot{\mathbf{q}}_{\mathrm{G}}$ as the column matrix of group velocities. By means of the coordinate partition method, the dependent accelerations might be expressed in terms of $\dot{\mathbf{q}}_{\mathrm{G}}$ and the independent accelerations $\ddot{\mathbf{h}}$. If no redundant constraint equations exists ($p = r$) the solution to the acceleration problem is expressed as:

$$\boldsymbol{\Phi}_{\boldsymbol{\varphi}}\ddot{\boldsymbol{\varphi}} + \boldsymbol{\Phi}_{\mathbf{h}}\ddot{\mathbf{h}} + \dot{\boldsymbol{\Phi}}_{\mathbf{q}_{\mathrm{G}}}\dot{\mathbf{q}}_{\mathrm{G}} + \dot{\boldsymbol{\Phi}}_{t} = \mathbf{0} \tag{30a}$$

$$\boldsymbol{\Phi}_{\boldsymbol{\varphi}}\ddot{\boldsymbol{\varphi}} = -(\boldsymbol{\Phi}_{\mathbf{h}}\ddot{\mathbf{h}} + \dot{\boldsymbol{\Phi}}_{\mathbf{q}_{\mathrm{G}}}\dot{\mathbf{q}}_{\mathrm{G}} + \dot{\boldsymbol{\Phi}}_{t}) \tag{30b}$$

Where $\dot{\boldsymbol{\Phi}}_{\mathbf{q}_{\mathrm{G}}}$ is the time derivative of the Jacobian matrix of the constraint equations derivated with respect the group coordinates $\mathbf{q}_{\mathrm{G}}$. Once again, the most efficient numerical methods, according to the size of the matrices in Eq.(30b) must be considered. For the example of the SG in Fig.4, matrix $\dot{\boldsymbol{\Phi}}_{\mathbf{q}_{\mathrm{G}}}\dot{\mathbf{q}}_{\mathrm{G}}$ is shown in Eq.(31).

$$\dot{\boldsymbol{\Phi}}_{\mathbf{q}_{\mathrm{G}}}\dot{\mathbf{q}}_{\mathrm{G}} = \begin{bmatrix} 2\left(\dot{x}_C - \dot{x}_A\right)\dot{x}_C + 2\left(\dot{y}_C - \dot{y}_A\right)\dot{y}_C - 2\left(\dot{x}_C - \dot{x}_A\right)\dot{x}_A - 2\left(\dot{y}_C - \dot{y}_A\right)\dot{y}_A \\ 2\left(\dot{x}_C - \dot{x}_B\right)\dot{x}_C + 2\left(\dot{y}_C - \dot{y}_B\right)\dot{y}_C - 2\left(\dot{x}_C - \dot{x}_B\right)\dot{x}_B - 2\left(\dot{y}_C - \dot{y}_B\right)\dot{y}_B \end{bmatrix} \tag{31}$$

In the most general case, redundant constraint equations appear ($p > r$) and Eq.(30b) must be redefined as:

$$\boldsymbol{\Phi}_{\boldsymbol{\varphi}}^{\mathrm{T}}\boldsymbol{\Phi}_{\boldsymbol{\varphi}}\ddot{\boldsymbol{\varphi}} = -\boldsymbol{\Phi}_{\boldsymbol{\varphi}}^{\mathrm{T}}(\boldsymbol{\Phi}_{\mathbf{h}}\ddot{\mathbf{h}} + \dot{\boldsymbol{\Phi}}_{\mathbf{q}_{\mathrm{G}}}\dot{\mathbf{q}}_{\mathrm{G}} + \dot{\boldsymbol{\Phi}}_{t}) \tag{32}$$

Option 2: third-order tensor approach. If the velocity coefficient matrix $\mathbf{K}_{\boldsymbol{\varphi}\mathbf{h}}$ has been obtained at the velocity stage, a more involved analysis has to be performed to derive the acceleration equations. Considering that a structural group is defined by r dependent and s independent group coordinates, and deriving both terms in Eq.(26) with respect to time, the acceleration problem can be formulated. Lets start with structural groups without redundant constraints:

$$\ddot{\boldsymbol{\varphi}} = \mathbf{K}_{\boldsymbol{\varphi}\mathbf{h}}\ddot{\mathbf{h}} + \sum_{i=1}^{s} \dot{h}_i \frac{\mathrm{d}\,\mathbf{K}_{\boldsymbol{\varphi}\mathbf{h}}}{\mathrm{d}\,h_i}\dot{\mathbf{h}} + \dot{\mathbf{S}}\mathbf{b} \tag{33}$$

where the first addend represents the tangential component of the acceleration of the dependent group coordinates, the last addend corresponds to the rheonomous term, which can be obtained as:

$$\boldsymbol{\Phi}_{\boldsymbol{\varphi}}\mathbf{S}\mathbf{b} = \mathbf{b} \rightarrow \dot{\mathbf{S}}\mathbf{b} = -\mathbf{S}\dot{\boldsymbol{\Phi}}_{\boldsymbol{\varphi}}\mathbf{S}\mathbf{b} + \mathbf{S}\dot{\mathbf{b}} \tag{34a}$$

$$\dot{\mathbf{b}} = -\dot{\boldsymbol{\Phi}}_{t} \tag{34b}$$

and the intermediate addend in Eq.(33) corresponds to the velocity dependent terms of the accelerations, which have been obtained applying the chain rule of derivation. In the total derivative of the velocity coefficient matrix $\mathbf{K}_{\boldsymbol{\varphi}\mathbf{h}}$ with respect to each independent group coordinate (Eq.(33)) the dependency that exist among the dependent group coordinates with respect to the independent ones must be considered. Introducing the velocity coefficient derivative $\mathbf{L}_{\boldsymbol{\varphi}\mathbf{h}/h_i}$ (a third-order tensor) as the derivative of the velocity coefficient matrix $\mathbf{K}_{\boldsymbol{\varphi}\mathbf{h}}$ with respect to a given independent coordinate h_i:

$$\mathbf{L}_{\boldsymbol{\varphi}\mathbf{h}/h_i} = \frac{\mathrm{d}\,\mathbf{K}_{\boldsymbol{\varphi}\mathbf{h}}}{\mathrm{d}\,h_i} \tag{35}$$

Then, the solution to the acceleration problem Eq.(33) can be expressed as:

$$\ddot{\boldsymbol{\varphi}} = \mathbf{K}_{\boldsymbol{\varphi}\mathbf{h}}\ddot{\mathbf{h}} + \sum_{i=1}^{s} \dot{h}_i \mathbf{L}_{\boldsymbol{\varphi}\mathbf{h}/h_i}\dot{\mathbf{h}} + \dot{\mathbf{S}}\mathbf{b} \tag{36}$$

Calculating the velocity coefficient derivatives is the most complicated and time consuming part of this approach. From the definition of the velocity coefficient matrix $\mathbf{K}_{\boldsymbol{\varphi}\mathbf{h}}$ in Eq.(25a), taking the total derivative of both terms with respect to the independent group coordinate h_i allows us to obtain the definition for the derivative of the velocity coefficient as:

$$\frac{\mathrm{d}\,\boldsymbol{\Phi}_{\boldsymbol{\varphi}}}{\mathrm{d}\,h_i}\mathbf{K}_{\boldsymbol{\varphi}\mathbf{h}} + \boldsymbol{\Phi}_{\boldsymbol{\varphi}}\frac{\mathrm{d}\,\mathbf{K}_{\boldsymbol{\varphi}\mathbf{h}}}{\mathrm{d}\,h_i} = -\frac{\mathrm{d}\,\boldsymbol{\Phi}_{\mathbf{h}}}{\mathrm{d}\,h_i} \tag{37a}$$

$$\boldsymbol{\Phi}_{\boldsymbol{\varphi}}\mathbf{L}_{\boldsymbol{\varphi}\mathbf{h}/h_i} = -\left(\frac{\mathrm{d}\,\boldsymbol{\Phi}_{\mathbf{h}}}{\mathrm{d}\,h_i} + \frac{\mathrm{d}\,\boldsymbol{\Phi}_{\boldsymbol{\varphi}}}{\mathrm{d}\,h_i}\mathbf{K}_{\boldsymbol{\varphi}\mathbf{h}}\right) \tag{37b}$$

Using the following notation to express the total derivatives of the Jacobian matrices with respect to the independent group coordinate h_i:

$$\frac{\mathrm{d}\,\boldsymbol{\Phi}_{\boldsymbol{\varphi}}}{\mathrm{d}\,h_i} = \boldsymbol{\Phi}_{\boldsymbol{\varphi}/h_i};\ \frac{\mathrm{d}\,\boldsymbol{\Phi}_{\mathbf{h}}}{\mathrm{d}\,h_i} = \boldsymbol{\Phi}_{\mathbf{h}/h_i}; \tag{38}$$

Eq.(37b) may be expresed as:

$$\boldsymbol{\Phi}_{\boldsymbol{\varphi}}\mathbf{L}_{\boldsymbol{\varphi}\mathbf{h}/h_i} = -\left(\boldsymbol{\Phi}_{\mathbf{h}/h_i} + \boldsymbol{\Phi}_{\boldsymbol{\varphi}/h_i}\mathbf{K}_{\boldsymbol{\varphi}\mathbf{h}}\right) \tag{39}$$

If analytic expressions for the elements of the velocity coefficient matrix $\mathbf{K}_{\boldsymbol{\varphi}\mathbf{h}}$ have been obtained, as in the example of the 3R structural group in Eq.(27), then the elements of the RHS parenthesis in Eq.(39) can also be analytically obtained to reduce the computational effort during the analysis. As an example, according to Fig.4, the first column of the (2×4) velocity coefficient derivatives $\mathbf{L}_{\boldsymbol{\varphi}\mathbf{h}/x_A}$ of the velocity coefficient matrix $\mathbf{K}_{\boldsymbol{\varphi}\mathbf{h}}$ derivative with respect the independent group coordinate x_A has the following form (where χ is the same as Eq.(20b)):

$$\mathbf{L}_{\boldsymbol{\varphi}\mathbf{h}/x_A} = \frac{1}{\chi}\begin{bmatrix} (y_A - y_C)\left(2K^2_{\boldsymbol{\varphi}\mathbf{h}}(1,1) + 2K^2_{\boldsymbol{\varphi}\mathbf{h}}(2,1)\right) - (y_B - y_C)\left(2K^2_{\boldsymbol{\varphi}\mathbf{h}}(2,1) - 2K_{\boldsymbol{\varphi}\mathbf{h}}(1,1) + K_{\boldsymbol{\varphi}\mathbf{h}}(1,1)\left(2K_{\boldsymbol{\varphi}\mathbf{h}}(1,1) - 2\right) + 2\right) \\ (x_B - x_C)\left(2K^2_{\boldsymbol{\varphi}\mathbf{h}}(2,1) - 2K_{\boldsymbol{\varphi}\mathbf{h}}(1,1) + K_{\boldsymbol{\varphi}\mathbf{h}}(1,1)\left(2K_{\boldsymbol{\varphi}\mathbf{h}}(1,1) - 2\right) + 2\right) - (x_A - x_C)\left(2K^2_{\boldsymbol{\varphi}\mathbf{h}}(1,1) + 2K^2_{\boldsymbol{\varphi}\mathbf{h}}(2,1)\right) \end{bmatrix} \tag{40}$$

The rheonomous term in Eq.(33) may also be obtained in more general structural groups with redundant constraints in a similar way, now by deriving Eq.(28b) with respect to time. First we reorganize the equation Eq.(34a) as:

$$\boldsymbol{\Phi}_{\boldsymbol{\varphi}}^{\mathrm{T}}\boldsymbol{\Phi}_{\boldsymbol{\varphi}}\mathbf{S}\mathbf{b} = \mathbf{b} \tag{41}$$

and then we derive Eq.(41) with respect to time to obtain $\dot{\mathbf{S}}\mathbf{b}$:

$$\boldsymbol{\Phi}_{\boldsymbol{\varphi}}^{\mathrm{T}}\boldsymbol{\Phi}_{\boldsymbol{\varphi}}\dot{\mathbf{S}}\mathbf{b} = -\left[\left(\dot{\boldsymbol{\Phi}}_{\boldsymbol{\varphi}}^{\mathrm{T}}\boldsymbol{\Phi}_{\boldsymbol{\varphi}} + \boldsymbol{\Phi}_{\boldsymbol{\varphi}}^{\mathrm{T}}\dot{\boldsymbol{\Phi}}_{\boldsymbol{\varphi}}\right)\mathbf{S}\mathbf{b} + \dot{\mathbf{b}}\right] \tag{42a}$$

$$\dot{\mathbf{b}} = -\dot{\boldsymbol{\Phi}}_{\boldsymbol{\varphi}}^{\mathrm{T}}\boldsymbol{\Phi}_t - \boldsymbol{\Phi}_{\boldsymbol{\varphi}}^{\mathrm{T}}\dot{\boldsymbol{\Phi}}_t \tag{42b}$$

Also the velocity coefficients as defined in Eq.(28a) may be derived with respect to the independent group coordinate h_i to obtain the corresponding velocity coefficient derivatives as:

$$\mathbf{\Phi}_{\boldsymbol{\varphi}}^{\mathrm{T}}\mathbf{\Phi}_{\boldsymbol{\varphi}}\mathbf{L}_{\boldsymbol{\varphi}\mathbf{h}/h_i} = -\left[\left(\mathbf{\Phi}_{\boldsymbol{\varphi}/h_i}^{\mathrm{T}}\mathbf{\Phi}_{\boldsymbol{\varphi}} + \mathbf{\Phi}_{\boldsymbol{\varphi}}^{\mathrm{T}}\mathbf{\Phi}_{\boldsymbol{\varphi}/h_i}\right)\mathbf{K}_{\boldsymbol{\varphi}\mathbf{h}} + \mathbf{\Phi}_{\boldsymbol{\varphi}/h_i}^{\mathrm{T}}\mathbf{\Phi}_{\mathbf{h}} + \mathbf{\Phi}_{\boldsymbol{\varphi}}^{\mathrm{T}}\mathbf{\Phi}_{\mathbf{h}/h_i}\right] \tag{43}$$

D. Solve the kinematics of other points of interest. Apart from the dependent group coordinates $\boldsymbol{\varphi}$, needed to model each specific SG, the position, velocity and acceleration analysis of other entities of interest (points and vectors) pertaining to the bodies of the same SG might be necessary. Normally the coordinates of such entities should not be included in matrix $\boldsymbol{\varphi}$ to keep its size as reduced as possible. If the body is defined, for example, by one point and three vectors whose global and local cartesian coordinates are: $[\mathbf{r}_1, \mathbf{V}_1, \mathbf{V}_2, \mathbf{V}_3]$ and $\left[\overline{\mathbf{r}_1}, \overline{\mathbf{V}}_1, \overline{\mathbf{V}}_2, \overline{\mathbf{V}}_3\right]$ respectively, then the rotation matrix $\mathbf{A}$ of that body can be easily computed:

$$\mathbf{X} = \begin{bmatrix} V_{1\mathrm{x}} & V_{2\mathrm{x}} & V_{3\mathrm{x}} \\ V_{1\mathrm{y}} & V_{2\mathrm{x}} & V_{3\mathrm{x}} \\ V_{1\mathrm{z}} & V_{2\mathrm{x}} & V_{3\mathrm{x}} \end{bmatrix} \tag{44a}$$

$$\overline{\mathbf{X}} = \begin{bmatrix} \overline{V}_{1\mathrm{x}} & \overline{V}_{2\mathrm{x}} & \overline{V}_{3\mathrm{x}} \\ \overline{V}_{1\mathrm{y}} & \overline{V}_{2\mathrm{y}} & \overline{V}_{3\mathrm{y}} \\ \overline{V}_{1\mathrm{z}} & \overline{V}_{2\mathrm{z}} & \overline{V}_{3\mathrm{z}} \end{bmatrix} \tag{44b}$$

$$\mathbf{A} = \mathbf{X}\overline{\mathbf{X}}^{-1} \tag{44c}$$

and then, the global coordinates of any other vector of interest V from this body whose local coordinates are known $\overline{\mathbf{V}}$ can be calculated as:

$$\mathbf{V} = \mathbf{A}\overline{\mathbf{V}} \tag{45}$$

Moreover, the kinematics of any other point of interest, P can also be calculated introducing the transformation matrix $\mathbf{T}_{4\times4}$ of the body it belongs:

$$\mathbf{T} = \begin{bmatrix} \mathbf{A} & \mathbf{r}_1 \\ \mathbf{0} & 1 \end{bmatrix} \tag{46}$$

Then, making use of the homogeneous coordinates: $\overline{\mathbf{r}}_{\mathrm{p}}^{*} = \left[\overline{x}_{\mathrm{p}}^{*}\ \overline{y}_{\mathrm{p}}^{*}\ \overline{z}_{\mathrm{p}}^{*}\ 1\right]$ and $\mathbf{r}_{\mathrm{p}}^{*} = \left[x_{\mathrm{p}}\ y_{\mathrm{p}}\ z_{\mathrm{p}}\ 1\right]$ it is straightforward to calculate the position of the point of interest:

$$\mathbf{r}_{\mathrm{p}}^{*} = \mathbf{T}\overline{\mathbf{r}}_{\mathrm{p}}^{*} \tag{47}$$

The first and second time derivatives of the transformation matrices $\mathbf{A}$ and $\mathbf{T}$ can also be calculated provided that the velocities and accelerations of the cartesian coordinates of the entities that define the rigid body are included in $\boldsymbol{\varphi}$ and $\mathbf{h}$ and, therefore, they are known at any instant of time. Then, the velocity and the acceleration of any point P or vector V of interest can also be easily calculated by taking the first and second time derivative of Eq.(45) and Eq.(47) respectively.

4. Methodology

To study how the two topological formulations based on group equations perform, in terms of computational cost, two scalable MBS have been studied: the 2D four-bar linkage and the 3D slider-crank mechanism. On the one hand, scalable MBS allow us to control the number of constraint equations and coordinates that define the MBS and, on the other hand, the selected 2D and 3D mechanisms show that the topological formulation solves both planar and spatial MBS with structural groups of different complexity. Moreover, since the most important difference between the two topological formulations consists of the way they compute the velocity dependent component of the acceleration, in order to compare the performance of both topological approaches, a code that performs the operations involved in the calculation of this component of the acceleration will be launched, controlling the sizes of the sets of dependent and independent group coordinates.

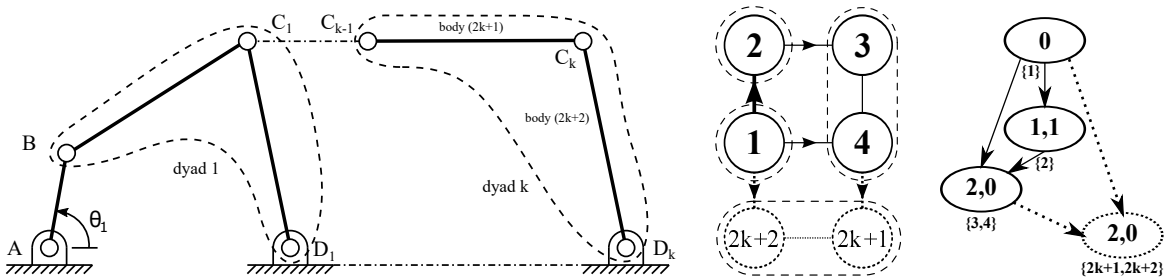

(a) Scheme of the mechanism. (b) Structural graph. (c) Structural diagram.

Figure 5: The scalable four-bar linkage is formed by a crank and a number of k dyads. Its kinematic structure is obtained by means of the structural graph and shown in its structural diagram.

Coordinates	**1R**	**Dyad 1: 3R**	**Dyad k: 3R**($\forall k > 1$)
Fixed coord.	$A(x, y)$	$D_1(x, y)$	$D_k(x, y)$
Indep coord.	θ_1	$B(x, y)$	$C_{k-1}(x, y)$
Dep coord.	$B(x, y)$	$C_1(x, y)$	$C_k(x, y)$

Table 1: Fixed, independent and dependent group coordinates of the structural groups: 1R, the first dyad 3R of the four-bar linkage and the rest of the k dyads 3R in case study 1.

4.1. Scalable 2D four-bar linkage

The scalable 2D four-bar linkage consists of a fixed frame (body 1), a crank (body 2, $\overline{AB}$), and an increasing number k of dyads that can be added to make this linkage scalable. Each one of these k dyads introduces two bodies: a rod (body $2k+1$,$\overline{C_{k-1}C_k}$), and a rocker (body $2k+2$, $\overline{C_kD_k}$) linked with an internal rotation joint C_k and attached to the previous dyad and the frame with two external rotation joints C_{k-1} and D_k (Fig.5(a)). All lengths are set equal to $6\,m$, except $\overline{AB} = 2\,m$.

The structural graph and the structural diagram associated to this linkage, obtained applying the methods exposed in section 3.2, are shown in Figs. 5(b) and 5(c) respectively. Once the frame has been isolated, the kinematic structure of this MBS is composed by: one SG, named 1R, formed by body 2 and one external rotation kinematic pair $\{1-2\}$, one dyad $\{3-4\}$, and a number of k ($\forall k > 1$) dyads, named 3R, formed by two bodies $(2k+1, 2k+2)$, whose kinematics can be solved in the order specified by the parameter k.

The constraint equations that define the two types of structural groups (1R and 3R) that conforms the scalable four-bar linkage are, respectively:

$$\mathbf{\Phi}_{1\mathrm{R}} = \begin{bmatrix} \mathbf{r}_{\mathrm{BA}}^{\mathrm{T}}\mathbf{r}_{\mathrm{BA}} - L_{\mathrm{BA}}^2 \\ x_{\mathrm{B}} - x_{\mathrm{A}} - L_{\mathrm{BA}}\cos\theta_1 \\ y_{\mathrm{B}} - y_{\mathrm{A}} - L_{\mathrm{BA}}\sin\theta_1 \end{bmatrix}_{3\times 1} \tag{48a}$$

$$\mathbf{\Phi}_{3\mathrm{R}} = \begin{bmatrix} \mathbf{r}_{\mathrm{CB}}^{\mathrm{T}}\mathbf{r}_{\mathrm{CB}} - L_{\mathrm{rod}}^2 \\ \mathbf{r}_{\mathrm{CD}}^{\mathrm{T}}\mathbf{r}_{\mathrm{CD}} - L_{\mathrm{rocker}}^2 \end{bmatrix}_{2\times 1} \tag{48b}$$

The first equation in column matrix $\mathbf{\Phi}_{1\mathrm{R}}$, express the rigid body condition for the crank, and the second and third equations are needed to introduce the relative coordinate θ_1. In each 3R structural group, $\mathbf{\Phi}_{3\mathrm{R}}$ include two rigid body conditions. The Jacobian matrices of each SG with respect to the dependent $\boldsymbol{\varphi}$ and independent $\mathbf{h}$ group coordinates can be easily obtained as:

$$\mathbf{\Phi}_{\boldsymbol{\varphi},\,1\mathrm{R}} = \left[\frac{\mathrm{d}\mathbf{\Phi}_{1\mathrm{R}}}{\mathrm{d}\boldsymbol{\varphi}_{1\mathrm{R}}}\right]_{3\times 2} \tag{49a}$$

$$\mathbf{\Phi}_{\mathbf{h},\,1\mathrm{R}} = \left[\frac{\mathrm{d}\mathbf{\Phi}_{1\mathrm{R}}}{\mathrm{d}\mathbf{h}_{1\mathrm{R}}}\right]_{3\times 1} \tag{49b}$$

Coordinates	**SG: 1R3D**	**Rod-slider k : SG: 2E1P ($\forall k \geq 1$)**
Fixed coord.	$A(x,y,z), V1(x,y,z), V3(x,y,z)$	$V6_k(x,y,z), V7_k(x,y,z), V8_k(x,y,z)$
Indep coord.	θ	$B(x,y,z), V4_k(z)$
Dep coord.	$B(x,y,z), V2(x,y,z)$	$C_k(x,y,z), V4_k(x,y), V5_k(x,y,z)$

Table 2: Fixed, independent and dependent group coordinates of the structural groups: $1R3D$ and the k ones of type $2E1P$ in case study 2.

$$\mathbf{\Phi}_{\boldsymbol{\varphi},\,3\mathrm{R}} = \left[\frac{\mathrm{d}\mathbf{\Phi}_{3\mathrm{R}}}{\mathrm{d}\boldsymbol{\varphi}_{3\mathrm{R}}}\right]_{2\times 2} \tag{49c}$$

$$\mathbf{\Phi}_{\mathbf{h},\,3\mathrm{R}} = \left[\frac{\mathrm{d}\mathbf{\Phi}_{3\mathrm{R}}}{\mathrm{d}\mathbf{h}_{3\mathrm{R}}}\right]_{2\times 4} \tag{49d}$$

4.2. Scalable 3D crank-slider mechanism

The scalable 3D crank-slider mechanism Fig.6(c) consists of a fixed frame (body 1), a crank (body 2, $\overline{AB}$) which rotates with respect to the frame, and an increasing number k of dyads that can be added to make this linkage scalable. Each one of these k dyads introduces two bodies: a rod (body $2k+1$, $\overline{B_kC_k}$), and a slider (body $2k+2$, D_k) which translates with respect to the frame at a fixed direction. Each rod is linked to the crank 2 and the corresponding slider by means of spherical joints. The length of the crank is set to $2\,m$ and the rods are set equal to $6\,m$. To set the degrees of freedom of the whole MBS to one: $L_c = 1$, the rotation of the rod with respect its longitudinal axis has been hindered by making the vertical component z of vector $\overrightarrow{V4}_k$ constant and equal to its value at the initial configuration.

The structural graph and the structural diagram associated to this linkage, obtained as exposed in section 3.2, are shown in Figs. 6(b) and 6(c) respectively. Once the frame has been isolated, the kinematic structure of this MBS is composed by: a first SG, named 1R3D, formed by body 2 and one external rotation kinematic pair $\{1-2\}$, and a number of k ($\forall k \geq 1$) dyads, named 2E1P, formed by two bodies $(2k+1, 2k+2)$, whose kinematics can be solved in the order specified by the parameter k. These structural groups have the coordinates shown in Table2.

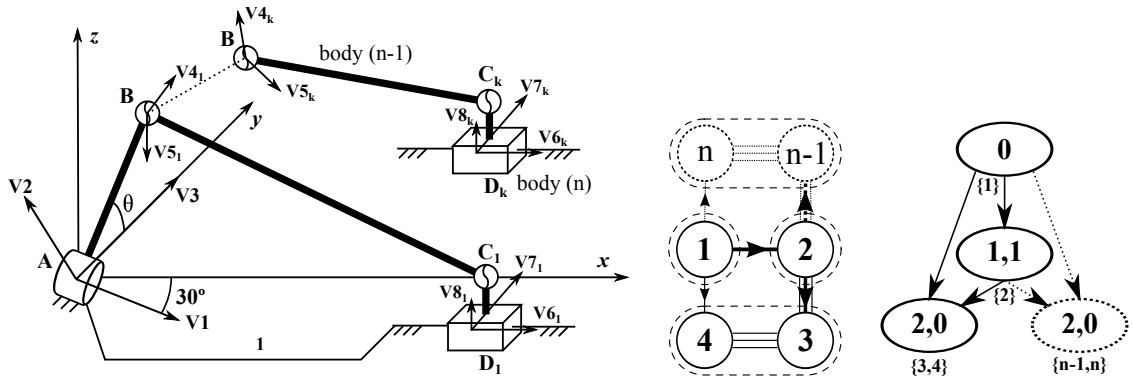

(a) Scheme of the mechanism. (b) Structural graph. (c) Structural diagram.

Figure 6: The scalable 3D slider-crank mechanism is composed by a crank and a number of k structural groups of type $2E1P$. Its kinematic structure is obtained by means of the structural graph and shown in its structural diagram.

The constraint equations associated to each SG are:

$$\mathbf{\Phi}_{\text{1R3D}} = \begin{bmatrix} \mathbf{r}_{\text{BA}}^{\text{T}}\mathbf{r}_{BA} - L_{\text{crank}}^2 \\ \mathbf{V}_2^{\text{T}}\mathbf{V}_2 - 1 \\ \mathbf{r}_{\text{BA}}^{\text{T}}\mathbf{V}_1 \\ \mathbf{r}_{\text{BA}}^{\text{T}}\mathbf{V}_2 \\ \mathbf{V}_1^{\text{T}}\mathbf{V}_2 \\ \mathbf{r}_{\text{BA}}^{\text{T}}\mathbf{V}_3 - L_{\text{crank}}\cos(\theta) \\ \mathbf{r}_{\text{BA}} \times \mathbf{V}_3 - L_{\text{crank}}\mathbf{V}_1\sin(\theta) \end{bmatrix}_{9\times 1} \tag{50a}$$

$$\mathbf{\Phi}_{\text{2E1P}} = \begin{bmatrix} \mathbf{r}_{\text{BC}}^{\text{T}}\mathbf{r}_{BC} - L_{\text{rod}}^2 \\ \mathbf{V}_4^{\text{T}}\mathbf{V}_4 - 1 \\ \mathbf{V}_5^{\text{T}}\mathbf{V}_5 - 1 \\ \mathbf{r}_{\text{BC}}^{\text{T}}\mathbf{V}_4 \\ \mathbf{r}_{\text{BC}}^{\text{T}}\mathbf{V}_5 \\ \mathbf{V}_4^{\text{T}}\mathbf{V}_5 \\ \mathbf{r}_{\text{CA}} \times \mathbf{V}_6 \end{bmatrix}_{9\times 1} \tag{50b}$$

In $\mathbf{\Phi}_{\text{1R3D}}$, the first equation corresponds to the rigid body condition of body 2, the second one defines $\mathbf{V}_2$ as an unitary vector and the three following equations define $\mathbf{r}_{\text{BA}}$, $\mathbf{V}_1$ and $\mathbf{V}_2$ as orthogonal vectors. The remaining equations are needed to introduce the relative coordinate θ.

The constraint equations $\mathbf{\Phi}_{\text{2E1P}}$ include a first equation that corresponds to the rigid body condition of the rod, the two following equations introduce $\mathbf{V}_4$ and $\mathbf{V}_5$ as unitary vectors, and the three last equations consider $\mathbf{r}_{\text{BC}}$, $\mathbf{V}_4$ and $\mathbf{V}_5$ as orthogonal vectors. The remaining equations define the prismatic kinematic pair {frame-slider}. The Jacobian matrices of each SG with respect to the dependent $\boldsymbol{\varphi}$ and independent $\mathbf{h}$ group coordinates can be easily obtained:

$$\mathbf{\Phi}_{\boldsymbol{\varphi},\,\text{1R3D}} = \left[\frac{\mathrm{d}\mathbf{\Phi}_{\text{1R3D}}}{\mathrm{d}\boldsymbol{\varphi}_{\text{1R3D}}}\right]_{9\times 6} \tag{51a}$$

$$\mathbf{\Phi}_{\mathbf{h},\,\text{1R3D}} = \left[\frac{\mathrm{d}\mathbf{\Phi}_{\text{1R3D}}}{\mathrm{d}\mathbf{h}_{\text{1R3D}}}\right]_{9\times 10} \tag{51b}$$

$$\mathbf{\Phi}_{\boldsymbol{\varphi},\,\text{2E1P}} = \left[\frac{\mathrm{d}\mathbf{\Phi}_{\text{2E1P}}}{\mathrm{d}\boldsymbol{\varphi}_{\text{2E1P}}}\right]_{9\times 8} \tag{51c}$$

$$\mathbf{\Phi}_{\mathbf{h},\,\text{2E1P}} = \left[\frac{\mathrm{d}\mathbf{\Phi}_{\text{2E1P}}}{\mathrm{d}\mathbf{h}_{\text{2E1P}}}\right]_{9\times 13} \tag{51d}$$

4.3. Computational kinematics: global and topological algorithms

The scalable MBS defined in the previous sections have been solved with two algorithms presented here: the first one deals with the kinematics of MBS using a global formulation while the second one uses a topological formulation based on group equations. Both algorithms are described using Fortran programming language.

In algorithm 1 the MBS is defined by n dependent coordinates $\mathbf{q}^{\text{d}}$ and f independent ones $\mathbf{q}^{\text{i}}$. These coordinates are related by m constraint equations $\mathbf{\Phi}(\mathbf{q}, t)$, and f driving constraints $\mathbf{\Phi}(\mathbf{q}^{\text{i}}, t)$ from which the set of independent coordinates can be evaluated at any instant of time.

Algorithm 1: Global solution.

1: `MBData` // read MultiBody model
2: for $t = t_0{:}\Delta t{:}t_f$ do
3: `evaluate`$(\mathbf{q}^{\mathrm{i}}, \dot{\mathbf{q}}^{\mathrm{i}}, \ddot{\mathbf{q}}^{\mathrm{i}})$ // independent coordinates from $\left[\boldsymbol{\Phi}^{\mathrm{D}}(\mathbf{q}^{\mathrm{i}}, t)\right]_{f\times 1}$
// Position problem
4: `evaluate`$(\boldsymbol{\Phi})$ // $[\boldsymbol{\Phi}(\mathbf{q}, t)]_{m\times 1}$ constraint equations
5: while $|\boldsymbol{\Phi}| > \epsilon$ do
6: `evaluate` $\boldsymbol{\Phi}_{\mathbf{q}^{\mathrm{d}}}$ // Jacobian $\boldsymbol{\Phi}_{\mathbf{q}^{\mathrm{d}}{}_{(m\times n)}}$
7: `solve` $\left(\boldsymbol{\Phi}_{\mathbf{q}^{\mathrm{d}}}\right)_{k-1}\left(\mathbf{q}^{\mathrm{d}}_{k} - \mathbf{q}^{\mathrm{d}}_{k-1}\right) = \boldsymbol{\Phi}_{k-1}$ // solve positions
8: `evaluate`$(\boldsymbol{\Phi})$
9: end
// Velocity problem
10: `evaluate`$(\boldsymbol{\Phi}_{\mathbf{q}})$ // Jacobian $\boldsymbol{\Phi}_{\mathbf{q}_{(m+f\times n+f)}}$
11: `solve` $\boldsymbol{\Phi}_{\mathbf{q}}\dot{\mathbf{q}} = -\boldsymbol{\Phi}_{t}$
// Acceleration problem
12: `evaluate` $\dot{\boldsymbol{\Phi}}_{\mathbf{q}}\dot{\mathbf{q}}$
13: `solve` $\boldsymbol{\Phi}_{\mathbf{q}}\ddot{\mathbf{q}} = -\dot{\boldsymbol{\Phi}}_{\mathbf{q}}\dot{\mathbf{q}} - \dot{\boldsymbol{\Phi}}_{t}$
14: end

The multibody model is read from a file and, at each time step (loop 2-14): the values of the independent coordinates are evaluated (line 3) from the set of $\boldsymbol{\Phi}^{\mathrm{D}}(\mathbf{q}, t)$ driving constraints. The position, velocity and acceleration problems are solved in lines: 5-9; 10-11 and 12-13 respectively, and finally, the time is increased by the time step defined for the analysis and the for-end loop is repeated until the final time is reached. The position problem uses an Newton-Raphson iterative method which lasts until the norm of the constraint equations falls below a predefined tolerance ϵ. It is clearly seen that in the global formulations, as the complexity of the MBS increases, the size of the matrices involved in the kinematic analysis increases accordingly.

Algorithm 1, which solves the kinematics of MBS based on a global formulation, have been implemented for two solutions: **GLOB** which considers dense matrices and uses libraries of linear algebra (Linear Algebra PACKage, also known as *LAPACK*, integrated in the Intel® Math Kernel Library MKL), and **GLOB_SP** which uses sparse subroutines (*MA27*, from the *Harwell Subroutine Library*, developed by the Numerical Analysis Group at the Rutherford Appleton Laboratory). Both global formulations are solved applying the time derivative approach.

Algorithm 2 solves the kinematic analysis by means of the topological approach based on group equations introduced in this paper. Once the model of the MBS has been read from a file, included its kinematic structure (MBData in line 1), the whole MBS is solved at each time step in a for-end loop (lines 2-14) until the final time of the simulation is reached. All the information related to the structural groups is stored in the data structure SG. At each time step, the values of the coordinates which are driven in the MBS are updated (line 3) from the corresponding driving constraints. Then, the MBS kinematics is solved in a new for-end loop (lines 4-13) in which each one of the SG is solved in the order (variable *ng*) specified by the MBS kinematic structure. The kinematic solution of each SG is obtained by calling specific subroutines, in a switch-case loop, in which the position, velocity and acceleration problems are solved as explained in section 3.3. Each time that a SG is solved, the global matrix *POI* is updated with the position, velocity and acceleration values of the coordinates of points and vectors of interest in the solved structural group.

Algorithm 2, for the modular topological formulation based on group equations, have been implemented for other two solutions: **MOD_TD** and **MOD_3OT** which corresponds to the time derivative approach and the third-order tensor approach respectively.

Algorithm 2: Topological SG solution, time derivative option.

```
1:  MBData;                          // read MultiBody model. Includes its kinematic structure
2:  for t = t_0 : Δt : t_f do
3:      evaluate(q^i, q̇^i, q̈^i)      // independent coordinates from [Φ^D(q^i, t)]_{f×1}
4:      for ng = 1 : length(SG) do
            // solve each SG as a subsystem
5:          switch SG(ng).type do
6:              case SG(ng).type == '1R' do
7:                  Solve_1R                                   // POI
8:              case SG(ng).type == '3R' do
9:                  Solve_3R                                   // POI
10:             case ... do
11:                 Solve ...                                  // POI
12:         end
13:     end
14: end
```

The three solutions have been implemented in Fortran 90 programming language, compiled with MS Visual Studio in RelWithDebInfo mode (in order to be able to register the computational cost of the different subroutines) and run on a Intel Core i5-2400 CPU 3.10 GHz, RAM 16 GB, and Windows7 SP1 64 bits. The Intel VTune Amplifier tool has been used to check the CPU time distribution among all the operations involved in the analysis.

5. Results and discussion

In this section the efficiency of two topological approaches based on group equations are studied in detail and compared with respect to a global formulation using the algorithms introduced in section 4.3.

5.1. Planar simulation results

As a first case study, the kinematic analysis (position, velocity and acceleration) of the scalable four-bar linkage shown in Fig.5(a) and described in section 4.1 is solved. The time loop is defined in the interval $[0-120]$ s with a time increment of $\Delta t = 0.005$ s so that the whole MBS is solved up to 24.000 times. At the initial time ($t_0 = 0$) the initial orientation of the crank is $\theta_o = \pi/2$ rad and during the time interval the angular velocity of the crank is set to a constant value: $\dot{\theta} = 34.96$ rad/s so that, at any instant of time, the independent coordinate can be evaluated as: $\theta = \dot{\theta}(t_F - t_0) + \theta_0$. An increment of $\Delta\theta = 10^\circ$ for the crank is obtained at each time step.

This test is launched with an increasing number of constraint equations n_{eq} which depends on the number of dyads k added to the scalable linkage, satisfying the relation: $n_{eq} = 2k + 2$. The number of constraint equations together with the CPU time consumed in each test and the speed up obtained for the different formulations are shown in table 3. Figure 7 shows the CPU time consumed by the four formulations: **GLOB**, **GLOB_SP**, **MOD_TD** and **MOD_3OT** defined in the previous section.

As it can be seen in Fig.7 the **GLOB** formulation shows a cubic response (the Matlab curve fitting tool shows a perfect adjustment, R = 1) on CPU time consumption as the number of constraint equations increases, whereas the other three approaches: **GLOB_SP**, **MOD_TD** and **MOD_3OT** show a linear behavior. From the speed-ups shown in Table 3 it can be clearly stated that: the topological approach **MOD_TD** performs $[61.0 - 27.0]$ times faster than the **GLOB_SP** and $[2.35 - 2.18]$ times faster than the **MOD_3OT** approach. Moreover, the **MOD_3OT** performs $[27.9 - 11.6]$ times faster than the **GLOB_SP**. It is also interesting to note that above a number of $n_{eq} = 62$ the speed ups stabilize at an almost constant value. These results have been confirmed by a series of test in which the number of constraint equations have been extended up to $n_{eq} = 2002$, which corresponds to the total number of 1000 dyads.

It is also interesting to point out that the '3R' dyads considered in this case study have two independent coordinates which coincides with the third dimension of the third-order tensor $L_{\varphi\mathbf{h}/h_i}$ so, due to the reduced size of the SG, the

nEq	Profiling (s)				Speed ups		
	GLOB	GLOB_SP	MOD_TD	MOD_3OT	$\frac{GLOB\_SP}{MOD\_TD}$	$\frac{GLOB\_SP}{MOD\_3OT}$	$\frac{MOD\_3OT}{MOD\_TD}$
22	0.746	0.976	0.016	0.035	61.0	27.9	2.18
42	2.171	1.823	0.049	0.112	37.2	16.3	2.28
62	4.198	2.509	0.087	0.205	28.8	12.2	2.35
82	7.059	3.124	0.119	0.269	26.3	11.6	2.26
102	11.036	4.502	0.156	0.348	28.9	12.9	2.23
122	16.696	5.108	0.180	0.416	28.4	12.3	2.31
142	24.694	6.021	0.205	0.475	29.4	12.7	2.31
162	33.221	6.814	0.252	0.563	27.0	12.1	2.23
182	44.466	7.981	0.284	0.642	28.1	12.4	2.26
202	57.139	8.715	0.317	0.718	27.5	12.1	2.26

Table 3: planar case: profiling and speed-ups of the four different approaches: global, global sparse, topological 'time derivative' and the so called topological 'third-order tensor' as a function of the number of constraints equations (nEq).

velocity coefficient matrix is given in symbolic form, and then, the only difference between the two topological approaches appears at the velocity dependent component of the acceleration, see Eq.(30a).

5.2. Spatial simulation results

The second case study is the kinematic analysis of the 3D crank-slider mechanism shown in Fig.6(a) and explained in subsection 4.2. The time loop is also defined in the interval $[0-120]\,s$ with a time increment of $\Delta t = 0.005 s$ so that 24.000 time steps of the whole MBS are solved. At the initial time ($t_0 = 0$) the initial orientation of the crank is $\theta_0 = 0\,rad$ and during the time interval the angular velocity of the crank is set to a constant value. In this case study, up to three angular velocities have been studied: $\dot{\theta} = \left[34.9E^{-5}, 34.9E^{-2}, 34.9\right]\,rad/s$ corresponding to three increments of $\Delta\theta = [0.0001°, 0.1°, 10°]$ for the rotation of the crank. This procedure allows us to evaluate the influence of the $\Delta\theta$ value in the number of iterations during the position problem.

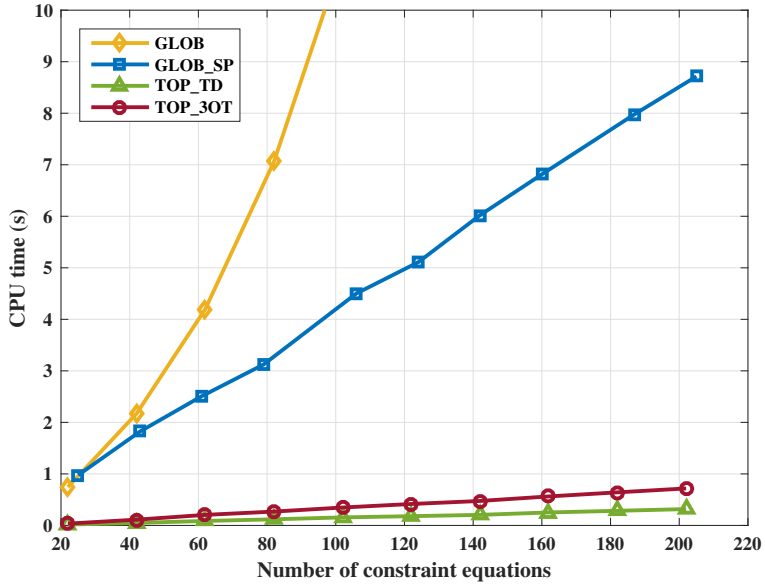

Figure 7: Planar case: evolution of the computational cost of the four approaches under study with the number of constraint equations (values from Table 3).

This is an scalable linkage in the sense that an increasing number of dyads (structural groups) formed by a rod and a slider can be attached at the point B of the crank with independence on the direction of the slider motion with respect to the frame. In this case, the number of constraint equations (n_{eq}) of the MBS is related to the number of dyads k considered in the study by means of the function: $n_{\text{eq}} = 8k + 6$. This MBS has been studied with the Global Sparse **GLOB_SP** and the two topological approaches: **MOD_TD** and **MOD_3OT**. The global approach with dense solver (**GLOB**) has not been considered due to the poor results obtained in the planar case.

As a first result, the horizontal component of the acceleration of the slider versus the crank rotation is shown in Fig.8(a) for the global sparse **GLOB_SP** and the two topological approaches: **MOD_TD** and **MOD_3OT**. The absolute values of the differences between the global approach and each one of the topological approaches are represented in Fig.8(b) for each kinematic problem: position, velocity and acceleration analysis, and for $[0° - 180°]$ crank angles. The biggest error is found in the position problem, having an order of magnitude of 10^{-13} for both topological solutions. The results offered by the three solutions are, then, very similar.

The computational cost of the **GLOB_SP** approach together with the speed ups of the **MOD_TD** and **MOD_3OT** approaches with respect the former are shown in Table 4 with different number of constraint equations for the three angular velocities considered: $\dot{\theta} = \left[34.9E^{-5}, 34.9E^{-2}, 34.9\right]$. It is important to note that, in the modular approaches, the kinematics of the SG have been solved by means of the LAPACK MKL libraries, which means that the matrices have been considered to be dense. However, the size of the matrices $\mathbf{\Phi}_{\boldsymbol{\varphi},\,1\text{R3D}}(9 \times 6)$, $\mathbf{\Phi}_{\mathbf{h},\,1\text{R3D}}(9 \times 10)$, $\mathbf{\Phi}_{\boldsymbol{\varphi},\,2\text{E1P}}(9 \times 8)$, $\mathbf{\Phi}_{\mathbf{h},\,2\text{E1P}}(9 \times 13)$ involved in the analysis of this case study are small enough to obtain a linear growth of the CPU time with respect to the number of constraint equations considered. It would be interesting to study how different solvers, dense and sparse, perform using the modular approach based on group equations depending on the size of the SG.

As expected, the CPU time spent by the global solutions in the planar and the spatial cases shows a similar value for the same number of constraint equations, being these ratios **GLOB_SP (3D/2D)** = 1.4. However, in spite of the linear growth of the topological approaches in the spatial case, the CPU time spent by these two solutions is higher than in the planar case, being their ratios: **MOD_TD (3D/2D)** = 12 and **MOD_3OT (3D/2D)** = 57 respectively.

From the results shown in Table 4, the **MOD_TD** approach shows speed ups with respect to the **GLOB_SP** one that ranges from $[2.248 - 3.18]$ for $\dot{\theta} = 34.9E - 5$ and similar speed ups, from $[2.326 - 3.166]$ for $\dot{\theta} = 34.9E - 2$. Better results have been obtained for $\dot{\theta} = 34.9$ which ranges from $[2.706 - 3.706]$. That means that when the value of the independent coordinate is considerably increased at each time step, the global formulation needs more iterations to achieve convergence than the topological ones.In all cases, the **MOD_3OT** shows a poor performance in this 3D study, with speed-ups that ranges from $[0.121 - 0.339]$.

It has been proved that the size of the matrices which define the structural groups affects the performance of the

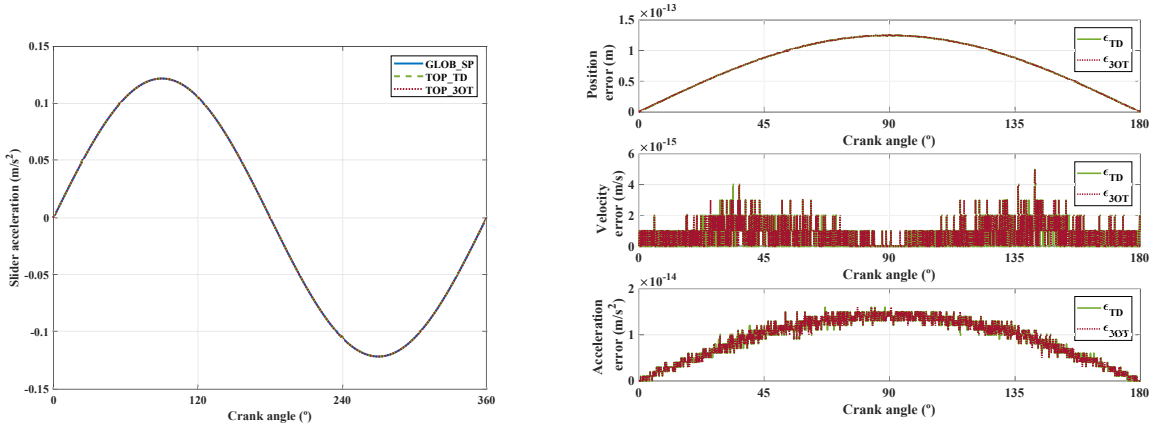

(a) Horizontal component of the acceleration of the slider vs crank rotation; results obtained by using three approaches: **GLOB_SP**, **MOD_TD** and **MOD_3OT**.

(b) Results for position (up), velocity (middle) and acceleration (down): comparison of differences of topological formulation with the global one $\epsilon_{TD} = |GLOB\_SP - MOD\_TD|$ and $\epsilon_{3OT} = |GLOB\_SP - MOD\_3OT|$.

Figure 8: Spatial case: comparative of the acceleration results of global and topological formulations.

nEq	Profiling (s)			Speed-ups					
	GLOB_SP			$\frac{GLOB\_SP}{MOD\_TD}$			$\frac{GLOB\_SP}{MOD\_3OT}$		
	34.9E-5	**34.9E-2**	**34.9**	**34.9E-5**	**34.9E-2**	**34.9**	**34.9E-5**	**34.9E-2**	**34.9**
14	0.281	0.435	0.717	2.248	2.326	2.706	0.121	0.181	0.280
86	1.981	2.870	4.632	2.593	2.390	2.856	0.119	0.170	0.274
166	3.946	5.771	9.655	2.456	2.623	3.207	0.125	0.178	0.298
246	5.974	8.688	13.977	2.715	2.579	3.200	0.131	0.183	0.277
326	8.408	12.090	19.623	2.821	2.636	3.364	0.136	0.195	0.296
406	10.372	15.084	24.616	2.782	2.686	3.287	0.138	0.194	0.298
486	12.745	18.673	29.873	2.918	2.830	3.520	0.142	0.202	0.302
566	15.849	22.432	37.080	3.070	2.953	3.548	0.147	0.204	0.319
646	18.205	26.924	43.303	3.146	2.935	3.691	0.152	0.219	0.339
726	21.013	30.123	48.343	3.082	3.022	3.672	0.150	0.209	0.326
806	23.758	33.929	54.629	3.180	3.166	3.706	0.156	0.217	0.339

Table 4: Spatial case: profiling of the global sparse approach and speed ups obtained by the two topological approaches, as a function of the number of constraint equations, for three constant angular velocities of the crank.

topological approaches and, moreover, in the case of the third-order tensor approach, the increase in the size of the number of independent coordinates in the structural group $2E1P$ worsens the efficiency of the decomposition into structural groups.

5.3. Profiling during the kinematic analysis of MBS.

Fig.9 and Table 5 show the distribution into the tasks in which the CPU time is mainly spent during the kinematic analysis of the spatial case study: the total **CPU time**, the CPU time spent in **Position**, **Velocity** and **Acceleration** analysis, and **Other** processes like building the multibody model or internal math operations of minor relevance. The results have been plot in a logarithmic bar graph for a better comparison of the different formulations. Solving the position, velocity and acceleration problems for the global **GLOB_SP** formulation takes the 77.7%, 17.6% and 2.7% of the whole CPU time respectively. For the **MOD_TD** these percentages are 94.5%, 1.7% and 3.4%. Finally for the **MOD_3OT** approach are 8.6%, 6.1% and 80.8%.

The position problem takes the same time for both topological approaches since they use exactly the same formulation and the same size of the matrices involved in the analysis. The global sparse formulation **GLOB_SP** is 3 times slower solving the position problem than the former two because it has to deal with matrices whose size equals the size of the whole MBS. In the velocity analysis, **MOD_TD** is about 38.7 times faster than **GLOB_SP** for the same reason that the position problem and 39.3 times faster than **MOD_3OT** since the matrix $\left(\mathbf{K}_{\boldsymbol{\varphi}\mathbf{h}}\right)$ has to be obtained by solving as many position problems as independent group coordinates define the structural group under analysis, as defined in Eq.(25a). Finally, in the acceleration problem, the global formulation **GLOB_SP** is three times slower than the time derivative approach **MOD_TD**, while the third-order tensor approach **MOD_3OT** spends up to a 80.8% of the whole CPU time performing this analysis due to the sum needed to compute the coefficient velocity derivatives $\boldsymbol{L}_{\boldsymbol{\varphi}\mathbf{h}/h_i}$, as defined in Eq.(37b).

	GLOB_SP	MOD_TD	MOD_3OT
Total	54.629	14.742	161.045
Position	42.431	13.931	13.853
Velocity	9.640	0.249	9.781
Acceleration	1.451	0.499	130.170
Others	1.107	0.063	7.241

Table 5: Spatial case: Profiling (ms) of the main stages of the kinematic analysis for the global sparse formulation and the two topological approaches at $nEq = 806$.

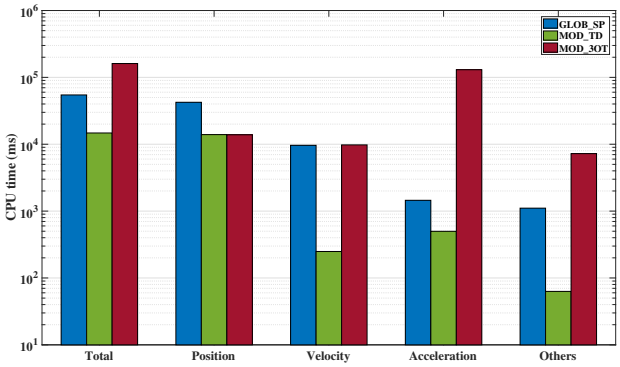

Figure 9: Bar graph representation of values from Table 5.

5.4. Results related to the implementation of the global and the modular solutions

The scalable four-bar and the 3D slider-crank linkages are formed by adding to a rotating crank as many SG of a certain type (3R and 2E1P respectively) to achieve an increasing number of coordinates and constraint equations. When dealing with the code needed to perform the studies, the modular approach allows us to list some advantages with respect to the global methods:

Modularity: the topological method based on group equations is a modular approach. The kinematic analysis of each SG can be programmed, optimized and compiled in an independent subroutine which might be included in a extensive library of structural groups. This modularity offers several advantages: facilitates the modeling and solution of any MBS, the analysis is fast and reliable and this library can be shared among other research groups.

Flexibility: the subroutines responsible for modeling and solving the kinematics of any SG might use any kind of coordinates (reference point, relative, natural or mixed coordinates). This feature is of interest because any analyst might use this more efficient approach without the necessity to introduce any change in the way they model or had modeled their MBS.

Performance: since the subroutine for the kinematic analysis of each SG might be solved with independence from the others, the efficiency of each subroutine can be improved by selecting the most appropiated solver depending on the topology of each SG. Moreover, the efficiency of the whole solution can be improved, depending on the kinematic structure of the MBS by exploiting hybrid parallelism in high performance computers (HPC) as shown in [43].

6. Conclusions

Computational methods for the kinematic analysis of multibody systems are a constant field of research because, in addition to being the base of dynamic analysis, these methods deal with many others problems of interest for the scientific community: angle and force transmission, range of motion, dimensional synthesis, inverse kinematics and control among others.

In this work, two formulations for the computational kinematics of multibody systems based on a modular approach in natural coordinates have been introduced. A mobility based algorithm is used for the structural analysis of multibody systems whichs allows us to obtain the kinematic structure of the multibody system under study. The kinematic structure shows the division of the multibody system into an ordered set of kinematically determined chains, or modules, which are used in the modular approach to solve the kinematics of the whole multibody system.

Then, two different formulations in natural coordinates which solve the kinematics of any kind of structural group by means of group equations have been introduced: the time derivative approach and the third-order tensor approach, whose main difference consist in the way they calculate the velocity dependent components of the accelerations. In order to evaluate the advantages of these topological approaches, they have been compared to a global formulation, also in natural coordinates, implemented with both dense and sparse solvers. In all cases the position problem is solved with iterative methods.

The performance of these four methods, in terms of computational cost, depending on the number of constraint equations of the MBS, has been analyzed by solving two case studies: the scalable four-bar linkage as a planar

mechanism, and the scalable 3D slider-crank linkage to prove that the topological formulations might also be applied to spatial MBS. Both case studies have been tested by increasing the number of structural groups to analyze their computational efficiency. The lack of efficiency of the global approach using dense matrices in the planar case study reveals unnecessary to apply this method in the three dimensional case.

6.1. Future developments

The topological formulation based on the kinematic structure of the MBS has shown many advantages with respect to global formulations. This fact encourages us to improve the possibilities it brings to the computational kinematic and dynamic analysis of MBS, as well as to solve its drawbacks.

Since this is a modular approach, the automatic modeling and solution of a MBS can be accomplished in two ways: by means of the offline use of symbolic software to feed with efficient and optimized solutions the kinematics solution subroutines of any SG, and by means of the use of the kinematic structure of the MBS, obtained by using computational methods, to automatically define the analysis sequence (automatic modeling of the MBS).

The modular character of this approach should be exploited to include the use of parallel calculation libraries combined with the use of different dense and sparse solvers to improve the efficiency of the calculations in kinematic and dynamic analysis of MBS.

Finally, a well known drawback related to all the topological formulations is that the efficiency of the solution, and even the capability to find a solution itself, depends on the kinematic structure of a MBS which might even change during the analysis. Methods devoted to find the more efficient kinematic structure and to allow the solution procedure to change to a different kinematic structure, at any time step, must be developed to make this formulation both efficient and general.

References

References

[1] A. A. Shabana, Dynamics of Multibody Systems, 2nd Edition, Cambridge Univ Press, 1998.
[2] M. Gerardin, A. Cardona, Flexible Multibody Dynamics: A finite element aproach, John Wiley & Sons, 2001.
[3] E. J. Haug, Computer-Aided kinematics and dynamics of mechanical systems, Allyn and Bacon, Boston, MA, 1989.
[4] P. E. Nikravesh, Computer aided analysis of mechanical systems, Prentice Hall, Englewood Cliffs, NY, 1988.
[5] J. García de Jalón, Kinematic and dynamic simulation of multibody systems, Springer-Verlag, NY, 1993.
[6] A. Rükgauer, W. Schiehlen, Simulation of modular dynamic systems, Mathematics and Computers in Simulation 46 (5) (1998) 535 – 542.
[7] R. Featherstone, A divide-and-conquer articulated-body algorithm for parallel O(log(n)) calculation of rigid-body dynamics Part 1: Basic algorithm, The International Journal of Robotics Research 18 (9) (1999) 867 – 875.
[8] R. Featherstone, A divide-and-conquer articulated-body algorithm for parallel O(log(n)) calculation of rigid-body dynamics Part 2: Trees, loops and accuracy, The International Journal of Robotics Research 18 (9) (1999) 876 – 892.
[9] J. H. Critchley, K. Anderson, A. Binani, An efficient multibody divide and conquer algorithm, in: Proceedings of the ASME 2007 International Design Engineering Technical Conferences & Computers and Information in Engineering Conference, Las Vegas, Nevada, USA, 2007.
[10] P. Malczyk, J. Frączek, A divide and conquer algorithm for constrained multibody system dynamics based on augmented lagrangian method with projections-based error correction, Nonlinear Dynamics 70 (1) (2012) 871–889.
[11] I. M. Khan, K. S. Anderson, A logarithmic complexity divide-and-conquer algorithm for multi-flexible-body dynamics including large deformations, Multibody System Dynamics 34.
[12] P. Malczyk, J. Frączek, F. González, J. Cuadrado, Index-3 divide and conquer algorithm for efficient multibody dynamics simulations, in: ECCOMAS Thematic Conference on Multibody Dynamics, Prague, Czech Republic, 2017.
[13] K. Singhal, H. Kesavan, Z. Ahmad, Vector-network models for kinematics: The 4-bar mechanism, Mechanism and Machine Theory 18 (5) (1983) 363 – 369.
[14] K. Singhal, H. Kesavan, Dynamic analysis of mechanisms via vector network model, Mechanism and Machine Theory 18 (3) (1983) 175 – 180.
[15] J. C. K. Chou, H. K. Kesavan, K. Singhal, A systems approach to three-dimensional multibody systems using graph-theoretic models, IEEE Transactions on Systems, Man, and Cybernetics 16 (2) (1986) 219 – 230.
[16] K. Arczewski, Graph theoretical approach - I. determination of kinetic energy for a class of particle systems, Journal of the Franklin Institute 329 (1992) 469–481.
[17] K. Arczewski, Graph theoretical approach - II. determination of generalized forces for a class of systems consisting of particles and springs, Journal of the Franklin Institute 329 (1992) 483–491.
[18] K. Arczewski, Graph theoretical approach - III. equations of motion of a class of constrained particle systems, Journal of the Franklin Institute 329 (3) (1992) 493 – 510.
[19] M. Richard, Dynamic simulation of multibody mechanical systems using the vector-network model, Transactions of the Canadian Society for Mechanical Engineering 12 (1) (1988) 21–30.

[20] A. Jain, Multibody graph transformations and analysis Part I: Tree topology systems, Nonlinear Dynamics 67 (4) (2012) 2779–2797.
[21] A. Jain, Multibody graph transformations and analysis Part II: Closed-chain constraint embedding, Nonlinear Dynamics 67 (3) (2012) 2153–2170.
[22] T. Kuroiwa, A. Motoe, H. Takahara, K. Hiraoka, Simulation system for the design of link mechanisms: Topological and kinematic analyses of mechanisms, JSME international journal 30 (268) (1987) 1652–1659.
[23] A. Kecskeméthy, On Closed Form Solutions of Multiple-Loop Mechanisms, Springer Netherlands, Dordrecht, 1993, pp. 263–274.
[24] P. Fanghella, Kinematics of single-loop mechanisms and serial robot arms: A systematic approach, Meccanica 30 (6) (1995) 685–705.
[25] A. Kecskeméthy, T. Krupp, M. Hiller, Symbolic processing of multiloop mechanism dynamics using closed-form kinematics solution, Multibody System Dynamics 1 (1) (1997) 23–45.
[26] J. J. McPhee, On the use of linear graph theory in multibody system dynamics, Nonlinear Dynamics 9 (1) (1996) 73–90.
[27] P. Shi, J. J. Mcphee, Dynamics of flexible multibody systems using virtual work and linear graph theory, Multibody System Dynamics 4 (2000) 355–381.
[28] P. Shi, J. J. Mcphee, Symbolic programming of a graph theoretic approach to flexible multibody dynamics, Mechanics of Structures and Machines 30 (1) (2002) 123–154.
[29] J. J. McPhee, C. Schmitke, S. Redmond, Dynamic modelling of mechatronic multibody systems with symbolic computing and linear graph theory, Mathematical and Computer Modelling of Dynamical Systems 10 (1) (2004) 1–23.
[30] J. Banerjee, J. McPhee, Graph-theoretic sensitivity analysis of multi-domain dynamic systems: theory and symbolic computer implementation, Nonlinear Dynamics 85 (1) (2016) 203–227.
[31] A. Kecskeméthy, M. Hiller, Automatic closed-form kinematics-solutions for recursive single-loop chains, in: Flexible mechanisms, Dynamic, and analysis, Washington, DC, USA, 1992, pp. 387–393.
[32] S. S. Kim, E. J. Haug, A recursive formulation for flexible multibody dynamics Part II: Closed loop systems, Computer Methods in Applied Mechanics and Engineering 74 (1989) 251–269.
[33] J. Samin, P. Fisette, Symbolic modeling of multibody systems, Kluwer Academic Publishers, 2003.
[34] A. Callejo, Y. Pan, J. Ricón, J. Kovecses, J. García de Jalón, Comparison of semirecursive and subsystem synthesis algorithms for the efficient simulation of multibody systems, Journal of Computational and Nonlinear Dynamics 12 (2016) 11–20.
[35] S. S. Kim, A subsystem synthesis method for efficient vehicle multibody dynamics, Multibody System Dynamics 7 (2) (2002) 189–207.
[36] X. Wang, J. K. Mills, Dynamic modeling of a flexible-link planar parallel platform using a substructuring approach, Mechanism and Machine Theory 41 (6) (2006) 671 – 687.
[37] S.-S. Kim, W. Jeong, Subsystem synthesis method with approximate function approach for a real-time multibody vehicle model, Multibody System Dynamics 17 (2) (2007) 141–156.
[38] S. S. Kim, C. H. Lee, A recursive subsystem synthesis method for repeated closed loop structure in multibody dynamics, Journal of Mechanical Science and Technology 23 (4) (2009) 946–949.
[39] J. Han, S.-S. Kim, W. Jeong, Subsystem synthesis method based on cartesian coordinates for unmanned military robot multibody dynamics model, in: 5th Asian Conference on Multibody Dynamics 2010, ACMD 2010, Vol. 1, 2010, pp. 317–324.
[40] P. Tomulik, J. Frączek, Simulation of multibody systems with the use of coupling techniques: a case study, Multibody System Dynamics 25 (2) (2011) 145–165.
[41] J. Buskiewicz, A method of optimization of solving a kinematic problem with the use of structural analysis algorithm (SAM), Mechanism and Machine Theory 41 (2006) 823–837.
[42] K. T. Wehage, R. A. Wehage, B. Ravani, Generalized coordinate partitioning for complex mechanisms based on kinematic substructuring, Mechanism and Machine Theory 92 (2015) 464 – 483.
[43] J. Cano, J. Cuenca, D. Gimenez, M. Saura, P. Segado, A parallel simulator for multibody systems based on group equations, The Journal of Supercomputing.
[44] G. Kinzel, C. Chang, The analysis of planar linkages using a modular approach, Mechanism and Machine Theory 19 (1984) 165–172.
[45] M. Smith, Z. Ye, Simplified data structure for analysing mechanisms using character handling techniques, Computer-Aided Design 16 (4) (1984) 197 – 202.
[46] J. N. Hammar, Considering cost effective computer-aided mechanism design, Computer-Aided Design 19 (10) (1987) 534 – 538.
[47] P. Fanghella, C. Galletti, A Modular Method for Computational Kinematics, Springer Netherlands, Dordrecht, 1993, pp. 275–284.
[48] M. Hansen, A general method for analysis of planar mechanisms using a modular approach, Mechanism and Machine Theory 31 (8) (1996) 1155–1166.
[49] J. R. M. Ho, Higher-order kinematic error sensitivity analysis and optimum dimensional tolerancing of dyad and non-dyad mechanisms, Master's thesis, University of Manitoba (1997).
[50] M. Z. Kolovsky, A. N. Evgrafov, Y. A. Semenov, A. V. Slousch, Advanced theory of mechanism and machines, Springer, 2000.
[51] M. Saura, A. Celdrán, D. Dopico, J. Cuadrado, Computational structural analysis of planar multibody systems with lower and higher kinematic pairs, in: Proceedings of the 2^{nd} Joint International Conference on Multibody System Dynamics, Stuttgart, Germany, 2012, pp. 376–377.
[52] G. Z. Baranov, A Course in the Theory of Mechanisms and Machines, Mir, 1988.
[53] M. Saura, A. Celdrán, D. Dopico, J. Cuadrado, Computational structural analysis of planar multibody systems with lower and higher kinematic pairs, Mechanism and Machine Theory 71 (2014) 79–92.
[54] M. Saura, P. Segado, D. Dopico, Formulaciones dinámicas en coordenadas naturales para la aproximación basada en ecuaciones de grupo, in: Proceedings of the XXI Congreso Nacional de Ingeniería Mecánica, Elche, Spain, 2016.
[55] S. Shah, S. Saha, J. Dutt, Modular framework for dynamic modeling and analyses of legged robots, Mechanism and Machine Theory 49 (2012) 234 – 255.
[56] W. A. Khan, C. P. Tang, V. N. Krovi, Modular and distributed forward dynamic simulation of constrained mechanical systems - A comparative study, Mechanism and Machine Theory 42 (5) (2007) 558 – 579.
[57] W. A. Khan, V. N. Krovi, S. K. Saha, J. Angeles, Modular and recursive kinematics and dynamics for parallel manipulators, Multibody System Dynamics 14 (3) (2005) 419–455.

[58] M. Koul, S.K., Saha, S. Shah, Reduced-order forward dynamics of multiclosed-loop systems, Multibody System Dynamics 31 (4) (2014) 451 – 476.

[59] P. Fanghella, C. Galletti, G. Torre, An explicit independent-coordinate formulation for the equations of motion of flexible multibody systems, Mechanism and Machine Theory 38 (5) (2003) 417 – 437.

[60] L. Romdhane, H. Dhuibi, H. B. H. Salah, Dynamic analysis of planar elastic mechanisms using the dyad method, Proceedings of the Institution of Mechanical Engineers, Part K: Journal of Multi-body Dynamics. 217 (2003) 1 – 14.

[61] J. García de Jalón, E. Bayo, Kinematic and dynamic simulation of multibody systems: The real-time challenge, Springer-Verlag, New York (USA), 1994.